FUNCTIONS OF PHOSPHATIDYLINOSITOL 4-PHOSPHATE 5 KINASES IN ACTIN CYTOSKELETAL REGULATION DURING PHAGOCYTOSIS

APPROVED BY SUPERVISORY COMMITTEE

Helen L. Yin, Ph.D. (Mentor)

Joseph P. Albanesi, Ph.D. (Chair)

Shmuel Muallem, Ph.D.

Michael G. Roth, Ph.D.

DEDICATION

I would like to thank my parents, Jun Dong and Heping Mao, for their unconditional love and continuous support.

FUNCTIONS OF PHOSPHATIDYLINOSITOL 4-PHOSPHATE 5 KINASES IN ACTIN CYTOSKELETAL REGULATION DURING PHAGOCYTOSIS

by

YUNTAO (STEVE) MAO

DISSERTATION

Presented to the Faculty of the Graduate School of Biomedical Sciences

The University of Texas Southwestern Medical Center at Dallas

In Partial Fulfillment of the Requirements

For the Degree of

DOCTOR OF PHILOSOPHY

The University of Texas Southwestern Medical Center at Dallas

Dallas, Texas

March, 2009

ACKNOWLEDGEMENT

It is my great pleasure to acknowledge the contributions of many people to this dissertation. First and foremost is my mentor, Dr. Helen Yin, who, in my humble opinion, is one of the top cell biologists. Your support, superb guidance, encouragement, inspiration, wisdom and constructive criticisms have been enormously benefitial to my professional career as well as my personal life. Thank you for your patience and trust.

The frequency with which I show the data of and I cite the publications of my many wonderful colleagues at Yin lab is indicatative of the great debt I owe them for their many contributions both scientifically and personally. Drs. Masaki Yamaga and Yongjie Wei contributed to the studies of RNAi in CHO-IIA cells and PIP5Ks tyrosine phosphorylation, respectively. Thank you for your generosity and wisdom throughout this project. I owe an equally amount of gratitude to Xiaohui Zhu, whose experimental skills are extraordinary and deeply appreciated. Without your help, I could not have done any of this. I have been very fortunate to have Dr. Susan Sun as my colleague, friend, and "family". You have provided terrific support, brought immeasurable joy, and contributed in ways too numerous to count. I am also greatly indebted to my friend and colleague, Anne Marie Corgan. Your suggestions and patience have been invaluable in improving this dissertation's quality and my professional career development. Dr. Dongmei Lu, I want to thank you for your friendship and encouragement. Thank you all for providing a lab atmosphere that truly makes coming to work every day a joy.

I must also take this opportunity to thank my marvelous colleagues at UT Southwestern, especially Dr. Barbara Barylko from Albanesi's lab, Yi Sun, Kent

Singleton, and Kole Roybal from Wuelfing's lab, Chengcheng Shen and Susan Lin from Hilgemann's lab, and Dr. Keng-Mean Lin from the Alliance. Drs. Joe Albanesi, Christoph Wuelfing, Chris Lu, Mike Bennett, and Don Hilgemann, I thank you all for your insightful comments, support and fruitful collaborations.

I could not have asked for a better thesis committee during my graduate studies. Dr. Joe Albanesi, the most knowledgeable person at UT Southwestern, you have always provided comfort, insights and patience and you are my inspiration in everything. Dr. Shmuel Muallem, thank you for your direction; you are a fantastic teacher with a big heart. Dr. Mike Roth, one of the most insightful scientists on the planet, your suggestions and vision are tremendous treasures to me. I want to express my profound gratitude to all of you for your direction throughout my thesis project as well as your support during my postdoc application process.

A number of important people at UT Southwestern have been responsible for helping and inspiring me along these years. In particular, Drs. Dick Anderson, Joel Goodman, Robin Hiesinger, Kate Luby-Phelps, Elliott Ross, Joachim Seemann and Paul Sternweis, have each made my graduate school life and my research richer and more complete.

I wish to acknowledge all of the administrative professionals for their invaluable professional assistance. Patsy Tucker and Carla Childers, I would like to thank you for offering me the most remarkable patience, kindness, and support I have ever known. Deborah Evalds and Nancy McKinney, I thank you for your helpful counseling and warm hospitality. You have transformed UT Southwestern from merely a school to a home.

FUNCTIONS OF PHOSPHATIDYLINOSITOL 4-PHOSPHATE 5 KINASES IN ACTIN CYTOSKELETAL REGULATION DURING PHAGOCYTOSIS

YUNTAO (STEVE) MAO, Ph.D.

The University of Texas Southwestern Medical Center at Dallas, 2009

MENTOR: HELEN L. YIN, Ph.D.

Phosphatidylinositol (4,5)-bisphosphate (PIP_2) is a crucial signaling phosphoinositide at the plasma membrane (PM) which mediates a variety of biochemical activities and cellular functions. It is primarily synthesized by type I phosphatidylinositol 4-phosphate 5-kinases (PIP5Ks) through the phosphorylation on the D-5 position of the inositol ring of phatidylinositol 4-phosphate [PI(4)P]. Mammals have three PIP5K isoforms named α, β, and γ (human isoform designation) which have a highly conserved central kinase homology domain and divergent amino and carboxyl terminal extensions.

There is now extensive evidence suggesting that PIP5Ks have unique functions and regulations in many cellular processes which provide the key to understand how functionally, and possibly physically, segregated PIP_2 pools are generated.

The actin cytoskeleton is dynamically remodeled during Fcγ receptor (FcγR)-mediated phagocytosis in a PIP_2-dependent manner. I investigated the role of PIP5Kγ and α isoforms, which synthesize PIP_2, during phagocytosis. *PIP5K*γ-/- bone marrow-derived macrophages (BMM) have a highly polymerized actin cytoskeleton and are defective in attachment to IgG-opsonized particles and FcγR clustering. Delivery of exogenous PIP_2 rescued these defects. PIP5Kγ knockout BMM also have more RhoA and less Rac1 activation and pharmacological manipulations establish that they contribute to the abnormal phenotype. Likewise, depletion of PIP5Kγ by RNA interference (RNAi) inhibits particle attachment. In contrast, PIP5Kα knockout or silencing has no effect on attachment but inhibits ingestion by decreasing Wiskott-Aldrich syndrome protein (WASP) activation and hence actin polymerization, in the nascent phagocytic cup. In addition, PIP5Kγ, but not α, is transiently activated by spleen tyrosine kinase (Syk)-mediated phosphorylation. I propose that PIP5Kγ acts upstream of Rac/Rho and that the differential regulation of PIP5Kγ and α allows them to work in tandem to modulate the actin cytoskeleton during the attachment and ingestion phases of phagocytosis.

TABLE OF CONTENTS

PRIOR PUBLICATIONS

Zheng J, Huang J, **Mao Y**, Liu S, Sun X, Zhu X, Ma T, Zhang L, Ji J, Zhang Y, Yin CC, Qiu X. (2009). Immunoglobulin gene transcripts have distinct VHDJH recombination characteristics in human epithelial cancer cells. *J Biol Chem*. (in pess).

Barylko B, **Mao YS**, Wlodarski P, Jung G, Binns DD, Sun H-Q, Yin YL, Albanesi JP. (2009). Palmitoylation controls the catalytic activity and subcellular distribution of phosphatidylinositol 4-kinase II α. *J Biol Chem*. (in pess).

Mao YS, Yamaga M, Zhu X, Wei YJ, Sun H-Q, Wang J, Yun M, Wang Y, Di Paolo G, Bennett M, Mellman I, Abrams CS, De Camilli P, Lu CY, Yin HL. (2009). Essential and unique roles of PIP5K-γ and -α in Fcγ receptor-mediated phagocytosis. *J Cell Biol*. 184 (2): 281-96.

Zhu X, Li C, Sun X, **Mao Y**, Li G, Liu X, Zhang Y, Qiu X. (2008). Immunoglobulin mRNA and protein expression in human oral epithelial tumor cells. *Appl Immunohistochem Mol Morphol.* 16(3):232-8.

Huang J, Sun X, **Mao Y**, Zhu X, Zhang P, Zhang L, Du J, Qiu X. (2008). Expression of immunoglobulin gene with classical V-(D)-J rearrangement in mouse brain neurons. *Int J Biochem Cell Biol.* 40(8):1604-15.

Mao YS, Yin HL. (2007). Regulation of the actin cytoskeleton by phosphatidylinositol 4-phosphate 5 kinases. *Pflugers Arch.* 455(1):5-18.

Qiu X, Zhu X, Zhang L, **Mao Y**, Zhang J, Hao P, Li G, Lv P, Li Z, Sun X, Wu L, Zheng J, Deng Y, Hou C, Tang P, Zhang S, Zhang Y. (2003). Human epithelial cancers secrete imunoglobulin G with unidentified specificity to promote growth and survival of tumor cells. *Cancer Res.* 63(19):6488-95.

LIST OF FIGURES

LIST OF TABLES

LIST OF DEFINITIONS

BCR – B cell receptor

BMM – bone marrow-derived macrophages

C3T – C3 transferase

CA – constitutively active

CR3 – complement 3 receptor

CSF – colony stimulating factor

DAG – diacylglycerol

DIC – differential interference contrast

DN – dominant negative

EGF – epidermal growth factor

ERK – extracellular signal-regulated kinase

FA – focal adhesion

FcεR – Fcε receptor

FcγR – Fcγ receptor

GEF – guanine nucleotide exchange factor

HPLC – High pressure liquid chromatograph

IC – immune complexes

IgG – immunoglobulin G

$InsP_3$ – inositol (3,4,5)-triphosphate

ITAM – immunoreceptor tyrosine-based activation motif

Jasp. – Jasplakinolide

KD – kinase dead

Latr. – Latrunculin

PA – phosphatidic acid

PH – Pleckstrin homology

PI3K – phosphoinositide 3 kinase

PI(4)P – phosphatidylinositol 4-phosphate

PIP – phosphatidylinositol monophosphate

PIP_2 –phosphatidylinositol (4,5)-bisphosphate

PIP_3 – phosphatidylinositol (3,4,5)-triphosphate

PIP5K – phosphatidylinositol 4-phosphate 5 kinase

PKA – protein kinase A

PLC – phospholipase C

PLD – phospholipase D

PM – plasma membrane

PV – pervanadate

pY – phosphotyrosine

RNAi – RNA interference

SRBC – sheep red blood cells

Syk – spleen tyrosine kinase

TCR – T cell receptor

TGN – *trans*-Golgi network

TLC – thin layer chromatograph

WASP – Wiskott-Aldrich Syndrome protein

WT – wild type

CHAPTER ONE
Introduction

PIP_2 DYNAMICS DURING PHAGOCYTOSIS

Fcγ receptor (FcγR)-mediated phagocytosis is critically important for innate host defense, inflammation and tissue remodeling (8). Professional phagocytes such as macrophages express FcγR to rapidly internalize opsonized pathogens and immune complexes (IC) (9). Phagocytosis involves spatially and temporally regulated steps including particle attachment, engulfment and phagosome maturation (8). Actin assembles at the nascent phagocytic cup and during cup extension and it disassembles during the completion of internalization (10). Like actin, the phosphatidylinositol 4,5-bisphosphate (PIP_2) level increases locally in the cup during ingestion and decreases prior to engulfment (11). The current paradigm is that PIP_2 synthesis promotes *de novo* actin polymerization to initiate particle ingestion, while PIP_2 elimination depolymerizes actin to promote closure of the phagocytic cup (12). Almost nothing is known about the role of PIP_2 and actin in the attachment phase.

PIP5KS DYNAMICS DURING PHAGOCYTOSIS

Since phagocytosis invokes temporally defined steps that are spatially confined to the phagocytic cup, it provides an exquisite model to examine the molecular mechanisms by which PIP_2 synthesis and dissipation are regulated within this restricted membrane structure (13). PIP_2 is synthesized primarily by the type I phosphatidylinositol

4-phosphate 5-kinases (hereafter referred to as PIP5Ks) and mammals have three isoforms named α, β and γ [reviewed in (14)]. PIP5Kγ has several splice variants (15) and the two major variants, γ87 and γ90, are functionally distinct; PIP5Kγ87 supports PLCβ-mediated Ca^{2+} signaling in HeLa cells (16), while PIP5Kγ90 is implicated in synaptic transmission, endocytosis and formation of focal adhesions (FAs) (6,17-20). There is emerging evidence from PIP5K RNA interference (RNAi) (16,21,22) and gene knockout (17,20,23-25) that the three PIP5K isoforms have unique roles in a tissue-specific manner. PIP5Kα (human isoform designation) has been implicated in FcγR-mediated phagocytosis (26), but the role of the other PIP5Ks has not been examined.

ESSENTIAL AND UNIQUE ROLES OF PIP5KS DURING PHAGOCYTOSIS

Here I show that PIP5Kγ and α are both recruited to the phagocytic cup but they regulate different steps in phagocytosis. PIP5Kγ promotes particle attachment by inducing controlled actin depolymerization to facilitate FcγR microclustering, while PIP5Kα promotes particle ingestion by activating the Wiskott-Aldrich Syndrome protein (WASP) to induce Arp2/3-dependent actin polymerization at the nascent phagocytic cup. In addition, I show that PIP5Kγ is rapidly and transiently activated by the spleen tyrosine kinase (Syk), while PIP5Kα is not. My findings establish that PIP5Kγ and α orchestrate different types of actin remodeling at sequential stages of phagocytosis. They also suggest that PIP5Kγ tyrosine phosphorylation initiates actin depolymerization to promote

FcγR microclustering during particle attachment and that it is tuned down to switch to net actin polymerization during the PIP5Kα-mediated ingestion step.

CHAPTER TWO
Review of the Literature

PHOSPHATIDYLINOSITOL 4-PHOSPHATE 5 KINASES

PIP_2 is particularly abundant at the PM and is proposed to be a PM organelle marker, which distinguishes the PM from the internal organelles that are more highly enriched in other types of phosphoinositides (27-29). As such, PIP_2 is the hub for the docking of multicomponent signaling complexes (30) and the maintenance of cytoskeletal-PM adhesion (31). PIP_2 is also a regulator of ion channels (32,33), endocytic and exocytic membrane trafficking (34,35), integrin signaling (36), cytokinesis (37), epithelial cell morphogenesis (38) and apoptosis (39,40). Some of these roles are mediated through PIP_2 dependent modulation of the actin cytoskeleton (41-43), while others are not (28). In addition, PIP_2 is the immediate precursor to three pivotal second messengers, diacylglycerol (DAG), inositol (1,4,5)-triphosphate ($InsP_3$), and phosphatidylinositol (3,4,5)-triphosphate (PIP_3) (44).

PIP_2 dynamics

PIP_2 is found primarily on the cytoplasmic leaflet of the PM, where it accounts for approximately 1% of membrane phospholipids (45). PIP_2 is generated from phosphatidylinositol monophosphates (PIPs) through two distinct pathways: first, by the type I PIP5Ks which phosphorylate PI(4)P on the D-5 position of the inositol ring, and second, by the type II PIP4Ks which phosphorylate PI(5)P at the D-4 position. These two types of PIP kinases are non-redundant, and have distinct functions (46). PIP4Ks exist as dimers which form a flattened surface that docks on the lipid bilayer (47).

PIP5Ks are likely to have a similar overall organization. Domain swapping experiments show that the recognition of PI(4)P vs. PI(5)P is dictated primarily by the specificity loop within the kinase core; PIP4Ks have a conserved Ala that recognizes PI(5)P, while PIP5Ks have a conserved Glu that recognizes PI(4)P (48). Since PI4P is much more abundant than PI(5)P (49), PIP5Ks are likely to be the major source of PIP_2. This is confirmed by pulse-labeling studies (50). I will focus on PIP5Ks exclusively in this dissertation.

PIP_2 level is determined by a balance between synthesis and dissipation. PIP_2 can be decreased in many ways. First, PIP_2 is hydrolyzed by phospholipase C (PLC) to generate $InsP_3$ and DAG. This provides an effective mechanism for downshifting the PIP_2 signal (51). Second, PIP_2 is converted by the class I phosphoinositide 3 kinases (PI3Ks) to generate PIP_3, which is important for signaling, growth regulation and cell migration (52,53). Third, the D-5 phosphate on the PIP_2 inositol ring is dephosphorylated by phosphoinositide 5 phosphatases (54), such as synaptojanin (55) and Ocrl (56), which have been implicated in the maintenance of PIP_2 homeostasis at the PM and *trans* Golgi network (TGN), respectively. Fourth, PIP_2 that is generated locally may be dissipated by diffusion, but a gradient can be maintained by continuous generation locally or by PIP_2 binding to scaffolding molecules at a site of synthesis to immobilize the lipid (13).

There is now overwhelming evidence suggesting that some pools of PIP_2 are generated in a spatially- and temporally-regulated manner, and that downregulation of the PIP_2 signal is critically important for the cycling of almost all PIP_2-dependent processes (57-59).

New tools for studying PIP_2 dynamics

Pleckstrin homology (PH)-PLCδ-GFP has been widely used to monitor PIP_2 dynamics in cells by high resolution live cell imaging (60). It strongly labels the PM (60) and its ability to accurately report PIP_2 levels at the PM, when overexpressed at low level, has been corroborated in fixed cells by using anti-PIP_2 antibody (27,61)

There have been many attempts to change the PIP_2 level in cells. A constitutively membrane targeted yeast inositol polyphosphate 5 phosphatase (Inp54p) is used to assess the role of PIP_2 in membrane-cytoskeleton interactions (62). A cell permeant PIP_2 binding peptide derived from gelsolin's PIP_2 binding domain depletes PM PIP_2 in 3T3-L1 adipocytes, and inhibits glucose transport in an actin-dependent manner (63). PIP_2 is shuttled into intact cells through histone carriers to increase PIP_2 globally (27) or selectively on the basal vs. apical side of polarized epithelial cells (38).

Recently, the arsenal for manipulating PIP_2 has become even more sophisticated. 5 phosphatase and PIP5K are targeted to the PM using the rapamycin-inducible FKBP and FRB dimerization (30,64,65). In one study, the cytosolic form of Inp54p is fused to CFP tagged FKBP (CFP-FKBP-Inp54p), and cotransfected with plasmids encoding FRB attached to the membrane targeting domain of Lyn11 (Lyn11-FRB), and YFP-PH-PLCδ (30). Rapamycin induces translocation of the normally cytosolic CFP-FKBP-Inp54p to the PM, and a reciprocal dissociation of YFP-PH-PLCδ from the PM. PIP_2 depletion by PM targeted Inp54p blocks the KCNQ K^+ channels, while rapamycin targeting of PIP5Kγ increases K^+ current. Significantly, targeting of an activator of PI3K, which increases PIP_3 but not PIP_2, has no effect on the K^+ channels. Since PIP_2 level is changed acutely in the absence of the cascade of Ca^{2+}, DAG or $InsP_3$ signals that normally accompany

PIP_2 signaling, these results show conclusively that PIP_2, and not the second messengers generated from PIP_2, is the direct regulator of the K^+ channels. This system has since been employed to show the role PIP_2 plays during many cellular processes including the gating of gap junction channels through connexin43 (66), the activation and recruitment of ERM (67) and receptor phosphorylation during Wnt signaling (68).

PH-PLCδ binds PIP_2 with high affinity, but it binds $InsP_3$, a product of PIP_2 hydrolysis, even more strongly (69). Therefore, in many cases, PH-PLCδ translocation measures the PIP_2 overall hydrolysis but does not directly reflect the PIP_2 reduction at the PM. Another probe, a mutant form (R332H) of the C-terminal domain of Tubby, has been developed to monitor PIP_2 dynamics (70). Tubby, unlike PH-PLCδ, does not bind $InsP_3$ significantly, nor is it affected by cytosolic Ca^{2+} change (71).

PIP_2 microdomains

It has been reported that approximately half of the cell's PIP_2 is synthesized preferentially in cholesterol/sphingolipid enriched caveolar light membrane fractions ("rafts") (72-74), and that these PIP_2-enriched microdomains exhibit locally regulated PIP_2 turnover and restricted diffusion-mediated exchanges with their environment (72). The PIP_2 at the rafts has been proposed to be responsible for the inhibition of γ-secretase (75) and has been shown to be required for the respiratory syncytial virus budding (76). There are also reports that PIP_2 is enriched in noncaveolar microdomains that are the staging platforms for choreographing signaling and cytoskeletal dynamics. The existence of PIP_2 microdomains is confirmed by immunofluorescence staining of PM sheets prepared from PC12 cells (77,78). The PM PIP_2 microdomains are heterogenous; some

contain conventional raft markers, while others are enriched for syntaxin, which is involved in Ca^{2+}-mediated exocytosis and mostly excluded from the low density raft fraction (77). Other PIP_2 clustering proteins have also been identified. These includes MARCKS, which sequesters PIP_2 under basal conditions, and is induced by agonist signaling to release PIP_2 for interaction with other PIP_2 targets (45) and GAP-43, which sequesters PIP_2 primarily in the rafts (79). In the case of phagocytosis, PIP_2 accumulates and remains in the phagocytic cup for minutes without diffusing away (13). This accumulation is not dependent on rafts or the actin cytoskeleton, raising the possibilities that lipids are held in place by the restriction caused by extreme membrane curvature and by binding to proteins within the phagocytic cup.

Raft isolation by floatation on density gradients shows that PIP5K is not enriched in rafts in PC12 cells or platelets (77,80), while the same PIP5K is recruited to lipid rafts during B cell activation (81). The yeast PIP5K, Mss4p, is also not present in rafts, although its association with membrane is sphingolipid dependent (82). Recently, the existence of rafts *per se* has been intensely debated (83), because there are suggestions that detergent extraction *per se* induces artifactual clustering, and optical measurements give mixed results, with only some data supporting the existence of a less mobile lipid population (84). A recent report provides a means to discriminate raft PIP_2 pools vs. non-raft PIP_2 pools in the cell by using raft-targeted (L_{10}-) and non-raft-targeted (S_{15}-) Inp54p, respectively (85). In this study, L_{10}-Inp54p-mediated depletion of raft PIP_2 in T cells resulted in a smooth phenotype void of membrane ruffles and filopodia. On the contrary, S_{15}-Inp54 depleted non-raft PIP_2 but increased raft PIP_2, which facilitates filopodia formation and cell spreading.

The questions of whether PIP_2 exists in heterogeneous microdomains, and whether these domains are formed by PIP_2 in cholesterol rich rafts by interaction with proteins, or by a combination of both, need to be answered. They hold the key to understanding how PIP_2 is regulated spatially and temporally, and how the PIP_2 pools generated by the PIP5K isoforms are functionally and possibly physically segregated.

PIP_2 regulates multiple actin binding proteins

Cytoskeletal proteins were among the first shown to be regulated by PIP_2 (41,42) and many of these proteins regulate actin dynamics at the cell cortex (86-88). Some bind PIP_2 through well defined PIP_2 recognition modules (89). For example, ezrin, a member of the ERM family which links actin filaments to the PM, has a FERM domain which binds PIP_2, inducing the relief of the autoinhibited state (90). However, the majority of actin regulatory proteins bind PIP_2 using less obviously structured motifs that contain clusters of basic/aromatic amino acids (41). Some examples are: WASP family proteins, which promote actin assembly by activating the nucleating Arp2/3 complex; gelsolin family proteins, which sever and cap actin filaments to promote dynamic actin reorganization; vinculin which regulates FA turnover; capping protein, which caps the (+) end of actin filaments; and cofilin, which severs actin filaments to accelerate their *in vivo* treadmilling. In most cases, PIP_2's charged inositol headgroup and hydrophobic acyl chain are both required for binding (91-93). The length of the acyl chain is also critical; di-C_{16} and di-C_8 PIP_2 bind cofilin while di-C_4 PIP_2 does not (93).

Recently, the three dimensional structure of cofilin bound to di-C_8 PIP_2 has been solved by NMR (93). It reveals rich mechanistic details about how cofilin interacts with

PIP_2, and suggests a model in which the interplay between cofilin inactivation by PIP_2 and activation by dephosphorylation can specify the spatial and temporal regulation of cofilin at the PM.

Cloning of PIP5Ks

Yeast has a single PIP5K gene, while mammals have three. In 1996, two mammalian PIP5K isoforms were cloned simultaneously from human and mice (94,95). These isoforms were independently named α and β, but unfortunately, the human and mouse isoform designations were reversed. That is, human PIP5Kα is equivalent to mouse β, and human PIP5Kβ is equivalent to mouse α. This disparate nomenclature has generated much confusion in the literature. *In this dissertation, I will use the human isoform designation exclusively* (Table 1). In 1998, a third isoform, named PIP5Kγ, was cloned (15), and it has splice variants that are functionally distinct (15,96). The EST database suggests that the α and β isoforms may also have alternative splice variants (95,97), but they have not been characterized functionally.

Table 1. Mammalian PIP5K isoforms and major splice variants

Human isoforms and splice variants	Mouse counterparts	Molecular weight (kDa)	Number of residues in human (mouse)
hPIP5Kα	mPIP5Kβ	68	549 (546)
hPIP5Kβ	mPIP5Kα	68	540 (539)
hPIP5Kγ87	mPIP5Kγ635	87	640 (635)
hPIP5Kγ90	mPIP5Kγ661	90	668 (661)
hPIP5Kγ93*	mPIP5Kγ688	93	NA (688)

* Not yet cloned or identified in humans.

The three PIP5K isoforms have a highly conserved central kinase homology domain which has approximately 80% sequence identity (Fig. 1). The PIP5Ks are

functionally similar in many respects. *In vitro*, they have similar enzyme kinetics and they are activated by phosphatidic acid (PA) (15,98), which is generated by phospholipase D (PLD) (99) or DAG kinase (100). In addition, all PIP5K isoforms are activated by Ser/Thr dephosphorylation (1,101), and by small GTPases such as RhoA (102), Rac1 (103), and Arf6 (104). PIP5Ks can be activated by sorting nexin 9 through its PX domain, which also mediates the targeting of sorting nexin 9 to the PM by binding to PIP_2. This provides an elegant positive feedback regulation during membrane invagination (105). When overexpressed, all can potentially cause trapping of membrane in recycling endosomes (57,106), form endosomal tubules (106), inhibit phagosome closure (59), generate actin comet tails (107) and prime secretory granules for exocytosis (97).

In addition, the PIP5K isoforms have divergent amino and carboxyl terminal extensions (Fig. 1). These regions are likely to be important for generating isoform-specific function and regulation (6,16-19,25,39,101). In this section, I will summarize what is known about the role of each PIP5K isoform and highlight their isoform-specific roles.

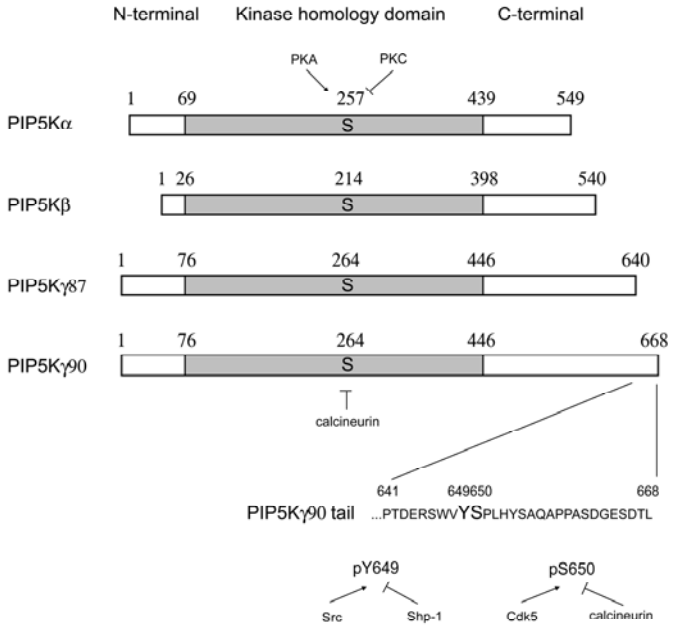

Figure 1. The domain structure of human PIP5K isoforms and their phosphorylation sites. PIP5Kγ has an 87 kDa isoform and a 90 kDa isoform which has a 28 amino acid extension at its C-terminus (tail). Ser257 in PIP5Kα (equivalent to Ser214 in β and Ser264 in γ) is constitutively phosphorylated by PKA or autophosphorylation, and it is dephosphorylated by a PKC-dependent pathway (1,2). Dephosphorylation activates the lipid kinases. In addition, the PIP5Kγ90 tail has two tandem phosphorylation sites (Tyr649 and Ser650), which are mutually exclusive. Tyr649 phosphorylation activates PIP5Kγ90 while Ser650 phosphorylation inhibits activity and blocks Tyr649 phosphorylation. Tyr649 is phosphorylated by Src (3) or EGFR (4) and dephosphorylated by Shp-1 (5). In neurons and neuroendocrine cells, PIP5Kγ90's Ser650 is phosphorylated by Cdk5, and dephosphorylated by calcineurin in response to K^+-induced depolarization (6,7).

PIP5K localization

PIP5Ks are cytosolic proteins that associate with the membrane as peripheral proteins. PIP5Kα, as well as the yeast and *Drosophila* orthologs, is also present in the nucleus (108). The mammalian PIP5K isoforms associate with the PM to a different

extent (97), and membrane association is regulated by multiple stimuli (109,110), especially Arf6, RhoA and Rac (41,111). In addition, isoform-specific binding partners that promote site-specific targeting have also been identified. Some examples are talin for PIP5Kγ90 (18,19), Ajuba (112) and Bruton's Tyr kinase (81) for PIP5Kα.

The PIP5K kinase homology domain is necessary for PM association (113), and the minimal targeting motif has been identified. These include two invariant Lys residues in the specificity loop, the conserved Glu that specifies PI(4)P recognition (114), and two tandem basic residues at the C-terminus of the kinase domain (113). These five residues are conserved in all known PIP5Ks from yeast to human, suggesting that they may be the universal PIP5K PM targeting code.

Non-mammalian PIP5Ks

PIP5Ks are found in yeast, *Arabidopsis*, *Drosophila* and *C. elegans*. Mss4p, the *S. cerevisiae* PIP5K, is particularly enriched at the PM (46,115). It clusters at sites of dynamic cortical assembly that are distinct from cortical actin patches, and the formation of these clusters is independent of actin filaments (116). Mss4p recruitment to the PM is dependent on normal sphingolipid biosynthesis, although it is not located in raft microdomains *per se* (82). *Mss4* mutants are unable to form actin cables, have abnormal distribution of actin patches, irregular cell shape, aberrant deposition of cell wall material, and decreased viability (46,117). These results establish that PIP_2 has important roles in *S. cerevisiae*, including the regulation of the actin cytoskeleton. The *S. pombe* PIP5K, Its3p, is also enriched at the PM. It regulates cell wall integrity of the fission

yeast through a PLC-mediated pathway (118), and it is concentrated at the septum during cytokinesis (119).

Drosophila has only one PIP5K gene. The partially characterized *Drosophila Sktl* is required for cell viability, germline development and bristle morphology (120). It has a nuclear localization signal, which shuttles Sktl between the nucleus and cytoplasm (121). Its nuclear localization suggests that it might be an ortholog of PIP5Kα, which is also found in the nucleus (108). Furthermore, since *Sktl* is not required for neurotransmitter release (120), it is not likely to be equivalent to mammalian PIP5Kγs, which have been strongly implicated in synaptic functions (18) (see below). *Sktl* has also been shown to be important for maintaining the cell polarity (122,123), the recruitment of Rab5 during clathrin-mediated endocytosis (124), and flagella biogenesis (125).

Mammalian PIP5Kβ

PIP5Kβ is ubiquitously expressed (94,95) and exists as a soluble protein in the cytoplasm, in association with punctate cytoplasmic structures and the PM (21,126). Initially, much of the information about PIP5Kβ was obtained by using transient transfection of wild type (WT) and kinase dead (KD) PIP5Kβ plasmids in cultured cells. There was no systematic attempt to distinguish between the function of individual PIP5K isoform. In some cases, the level of overexpression was unphysiologically high, overwhelming the normal mechanisms for specifying unique isoform functions. In addition, some of the putative KD mutants are not actually kinase dead, and most are not consistently dominant negative (DN) (Table 2). Nevertheless, in spite of these caveats,

there is convincing evidence that PIP5Kβ has a major role in actin regulation. Recently, RNAi and gene knockout by homologous recombination have provided definitive evidence for its isoform-specific function.

Table 2. Kinase dead mutants* used to probe PIP5K functions

Amino acid WT→KD	Residue number in human (mouse equivalent)	Function	References
K→A/M**	α181(179), β138(138), γ188(188)	Corresponds to the Lys in protein kinases that binds ATP's α-phosphate	(2,15,77,127-130)
D→A/N/V	α246(244), β203(203), γ253(253)	A putative substrate binding site	(5,19,129,131)
D→A	α270(268), β227(227), γ277(277)	A putative substrate binding site	(57,132-135)
D→K/N/A	α309(307), β266(266), γ316(316)	Corresponds to the catalytic Asp in protein kinases	(26,96,128,136,137)
R→Q	α427(425), β386(386), γ434(434)	?	(26,137,138)
truncation	αΔ1-240 (Δ1-238)	Dimerizes with WT PIP5K	(130,139,140)

* Most KD mutants do not consistently behave as DNs.

** This mutant has partial kinase activity when expressed in mammalian cells, and is therefore not a true KD mutant (26,132).

Regulation of actin polymerization

PIP5Kβ overexpression induces actin polymerization, but the type of actin filaments formed is dependent on the cells studied and the extent of overexpression (126,127,132,135,141). For example, PIP5Kβ overexpression induces the formation of

pine needle-like actin structures in COS-7 cells (126) and robust stress fibers in CV1 cells (132). The stress fibers are formed in a RhoA-dependent manner, by changing the activity of several PIP_2-sensitive actin regulatory proteins, including gelsolin, profilin, cofilin and erzin (132). PIP5Kβ is also implicated in RhoA-dependent ezrin recruitment to microvilli in HeLa cells (127) and Rac1-dependent recruitment to cell junctions (135).

Frequently, overexpression of PIP5Kβ, or the other PIP5K isoforms, induces the formation of actin comet tails that propel vesicles enriched with PIP5K and PIP_2 (107). Comet formation is WASP- and Arp2/3-dependent. These comets may be used for vesicle trafficking of "raft" associated cargoes from the TGN to the PM of nonpolarized cells (107), and selectively to the apical PM of polarized MDCK cells (142).

PIP5Kβ has also been implicated in neurite retraction downstream of RhoA and its effector, ROCK. PIP5Kβ overexpression in neuroblastoma N1E-115 cells induces neurite retraction even when ROCK is inactive; while overexpression of the PIP5Kβ KD mutant induces spontaneous neurite extension (136,143). PIP5Kβ may also be important for the phagocytosis of *Yersinia* (134); which binds to the host integrin β1 receptor to activate Rac1. Overexpression of either PIP5Kβ or Arf6 bypasses the Rac1 requirement, suggesting that they act downstream of Rac1 during *Yersinia* phagocytosis. Since FcγR-mediated phagocytosis is also regulated by Rac and Arf6 (144), the possibility that PIP5Kβ is also involved merits investigation.

The importance of PIP5Kβ in actin regulation is supported by gene knockout. Mast cells from the *PIP5Kβ*-/- (mouse *PIP5K*α-/-) mice have 35% less PIP_2 and less polymerized actin at the cell cortex (25). They have abnormally robust responses to Fcε

receptor (FcεR) I crosslinking, and hyperresponsiveness is supported by the finding that the *PIP5Kβ*-/- mice exhibit enhanced passive cutaneous and systematic anaphylaxis. Latrunculin (Latr.), which depolymerizes actin, increases degranulation and cytokine generation in WT mast cells, establishing that *PIP5Kβ*-/- phenotype can be directly attributed to decreased actin polymerization. Taken together, these results indicate that PIP5Kβ negatively regulates mast cell functions by maintaining a cortical actin network that dampens the dynamics of FcεR I signaling and downstream responses. Paradoxically, although *in vitro* and *in vivo* evidence suggest that PIP5Kβ has an important role in actin regulation, the *PIP5Kβ*-/- mice have no other reported phenotype. They are viable and develop normally (25). Furthermore, no compensatory change in the expression of the other PIP5Ks is detected.

Receptor-mediated endocytosis

PIP5Kβ also has roles that are not related to actin regulation. For example PIP5Kβ overexpression promotes receptor-mediated endocytosis in HeLa cells. These are manifested by an increase in transferrin uptake, the number of nascent clathrin-coated pits at the PM and the amount of membrane associated clathrin adaptor protein AP-2 complexes (21). Cytochalasin D or Latr. A, agents that depolymerize actin by different mechanisms, does not block the PIP5Kβ effects. Significantly, PIP5Kβ depletion by RNAi inhibits transferrin uptake in HeLa cells, while depletion of the other PIP5Ks has little effect (21). Taken together, these results establish that PIP5Kβ is the primary regulator of receptor-mediated endocytosis in HeLa cells. Neurons use another PIP5K

isoform to regulate endocytosis, although the mechanism for increased AP-2 recruitment may be similar (6,145).

Neutrophil polarity and directional movement

PIP5Kβ has been shown to be localized at the uropod of differentiated HL-60 cells and this localization does not require its lipid kinase activity but requires the last 83-aa C-terminal tail which is not present in other isoforms (146). This tail mediates the interaction between PIP5Kβ and EBP50, which enables further interaction with ERM and RhoGDI. These interactions provide a venue for PIP5Kβ to function as a scaffold to coordinate the rear signaling during leukocyte migration. Knockdown of PIP5Kβ impaired RhoA activation during neutrophil polarization suggesting that PIP5Kβ also acts upstream of and actively regulates Rho GTPases instead of being their downstream effector. In addition, another study showed that PIP5Kγ90 is enriched at the uropod of primary neutrophil and differentiated HL-60 cells during chemotaxis. This enrichment is required for PIP_2 generation at the uropod and the backness signaling during migration (147).

Wnt signaling

A study using human siRNA library screen identified that PI4KIIα and PIP5Kβ are among the proteins required for the canonical Wnt-β-catenine signaling pathway (68). Wnt3a stimulates the PIP_2 synthesis through frizzled and dishevelled and the latter

directly interacts and activates PIP5K activity. In turn, PIP_2 regulates LRP6 aggregation to axin microdomains and therefore, LRP6 phosphorylation.

Regulation by Rho and Arf family small GTPases

Now there is extensive evidence to suggest that PIP5Ks are regulated by RhoA, Rac1 and Arf6. RhoA and Rac1 have potent, and sometimes opposite, effects on the actin cytoskeleton and their ability to recruit and activate PIP5Ks provides a very attractive model for how they may regulate the actin cytoskeleton. This relation has been reviewed extensively (41,111,148) and will not be discussed further here.

Arf6, which regulates membrane trafficking between endosomes and the PM, has also been implicated in the regulation of cell motility and the actin cytoskeleton through PIP5Ks. Overexpression of the constitutively active (CA) Arf6 mutant or PIP5K induces trapping of PM-derived, PIP_2-rich vesicles in the recycling endosome compartment by polymerized actin (57). Honda et al. (104) reported that PIP5Kβ (as well as PIP5Kα) is recruited to membrane ruffles by Arf6, and that recombinant Arf6-GTP binds PIP5Kβ and stimulates its lipid kinase activity. Surprisingly, Rac1 and RhoA do not stimulate PIP5Kβ activity under similar conditions, even though they are reported to do so in other studies (102,149-151). The relation between Arf6 and PIP5K is further consolidated by the finding that Arf6 also recruits PLD2 to membrane ruffles (99,104). PLD has been intimately linked to PIP5Ks because it generates the PIP5K activator, PA (99) and, in addition, it is itself activated by PIP_2 (152,153). Thus, Arf6 recruitment of both PIP5Ks and PLD to membrane ruffles establishes a positive feedback loop between PIP5K and

PLD to synergistically amplify the initial Arf6 signal. There is now also evidence that Arf6 regulates PIP5Kγ in neurons and chromaffin cells to promote membrane trafficking and vesicle priming for exocytosis (137,154) (see below). In addition, Arf6 induces formation of endosomal tubules that contain PIP5Ks (106).

Although Arf6 is likely to be a primary regulator of PIP5K at the PM, some of the Arf6 responses may be coordinated with the activity of Rho GTPases, because Arf6 may act upstream or downstream of RhoA and Rac, depending on the cellular context. This web of interactions could involve elaborate positive and negative feedback loops that are only beginning to be understood.

Regulation by phosphorylation/dephosphorylation

a. Ser/Thr phosphorylation

Unexpectedly the PIP5Ks kinase core, which has no identifiable homology to any known protein kinase (155), can phosphorylate itself on Ser/Thr residues *in vitro* and phosphorylation inhibits lipid kinase activity (2). Although there is no evidence that PIP5K autophosphorylates in the context of the cell, this could explain why PIP5Ks are constitutively phosphorylated, and provide a mechanism to dampen basal PIP_2 generation under resting conditions. PIP5Ks' phosphorylation is also regulated by conventional kinases and phosphatases. The cAMP-dependent protein kinase A (PKA) phosphorylates PIP5Kβ *in vitro* (1) and the PKA phosphorylation consensus is located in the kinase homology domain. Mutation of Ser214 within the consensus (Fig. 1) to Ala decreases basal PIP5Kβ phosphorylation by 60% (1).

Stimuli that activate PIP5Kβ by Ser/Thr dephosphorylation have also been identified. Lysophosphatidic acid, which activates RhoA, induces PIP5K dephosphorylation in a PKC dependent manner in NIH 3T3 cells (1). Hypertonicity, which increases PIP_2 level and induces actin assembly in many types of cells, activates PIP5Kβ by dephosphorylation (101). In addition, hypertonicity also promotes PIP5Kβ association with the PM. Since neither actin disruption nor stabilization by pharmacological agents blocks PIP5Kβ dephosphorylation, PIP5Kβ is dephosphorylated upstream of actin remodeling. The RhoA effector, ROCK, is not involved, because the PIP5Kβ response is not blocked by a ROCK inhibitor. Significantly, PIP5Kα and γ, which are also constitutively Ser/Thr phosphorylated under isotonic conditions, are not dephosphorylated by hypertonicity. These results clearly establish that PIP5Kβ is regulated by a balance between protein kinase and phosphatase activity in response to hypertonic stress, and that the PIP5Ks have isoform-specific function and distinct modes of regulation.

b. Tyr phosphorylation

It has been known for some time that Tyr phosphorylation is involved in the control of PIP_2 homeostasis. Pervanadate (PV), a potent Tyr phosphatase inhibitor, increases PIP_2 in HEK293 and REF52 cells (107,156), while oxidative stress, which activates multiple Tyr kinases, decreases PIP_2 generation by isolated cardiac PM (157) and by HeLa cells (40). The paradox of how stimuli that promote Tyr phosphorylation have opposite effects on cellular PIP_2 can be explained. First, PIP5K isoforms are

expressed at different levels in different types of cells, and second, Tyr phosphorylation appears to have different effects on the PIP5Ks. PIP5Kγ90 is activated by Src kinases (19) (see below), while preliminary evidence suggests that PIP5Kβ is inhibited (40). PIP5Kβ inhibition is inferred from the finding that the PIP5Ks immunoprecipitated from H_2O_2-treated HeLa cells are less active *in vitro* than those from control cells (40). Although this antibody recognizes all PIP5K isoforms, PIP5Kβ should dominate in the immunoprecipitate, because it accounts for most of the PIP_2 in HeLa cells (16). Immunofluorescene studies also show that oxidative stress dissociates PIP5Kβ from the PM (40). Thus, the large decrease in PM PIP_2 in oxidant-stressed cells may be due to PIP5Kβ inactivation and dissociation from the PM. This decrease may be an early signal for apoptosis, because PIP5Kβ overexpression, which prevents oxidant-induced PIP_2 decrease, protects cells from apoptosis (40).

Mammalian PIP5Kγ

Unlike PIP5Kβ knockout, PIP5Kγ knockout mice die within a day of birth (17). The primary cause of death has not been determined, but may be due to generalized neuronal defects (see below), which are manifested in the inability to suckle and move normally. In another PIP5Kγ knockout mouse model, the *PIP5K*γ-/- mice embryos have myocardial developmental defects associated with impaired intracellular junctions that lead to heart failure and extensive prenatal lethality at embryonic day 11.5 of development (20). Humans have at least two major PIP5Kγ splice variants: a short 87 kDa protein (PIP5Kγ87), and a slightly longer one that has 28 additional amino acids at

its C-terminus (PIP5Kγ90) (15) (Fig. 1). PIP5Kγ87 is more abundant than PIP5Kγ90 in most cells (5,16,158,159), while PIP5Kγ90 dominates in the brain (18,160). Mice have an additional brain-specific 93 kDa splice variant which has not yet been described in humans (96). Since all three splice variants are knocked out in the currently available mouse models (17,20), it is difficult to attribute a defect to the knockout of a particular splice variant.

Focal adhesion dynamics

PIP_2 has long been implicated in the regulation of FAs, which are sites of actin filament attachment to the extracellular matrix through integrin receptors, and mediators of bidirectional integrin signaling (161). The PIP_2 level increases transiently during cell attachment to extracellular matrix, and PIP_2 activates several key FA components, including vinculin, α-actinin and talin. Although vinculin mutants that do not bind PIP_2 are recruited to FA normally, their FAs are static and turnover slowly (162,163). These results suggest that vinculin is a sensor of PIP_2 in the FA, and that it promotes dynamic FA assembly and disassembly. Talin, which binds vinculin, actin and integrin, has a key role in coupling the cytoskeleton to integrins (164). An early study suggests that PIP_2 promotes talin:integrin interaction (165). Now there is strong evidence that talin has a direct role in increasing PIP_2 at FA, because it binds to the carboxyl-terminal tail of PIP5Kγ90, and binding recruits PIP5Kγ90 to FA (18,19).

Talin:PIP5Kγ90 interaction is reciprocally regulated by phosphorylation of the tandem Tyr649 and Ser650 residues in PIP5Kγ90's talin binding tail (WV**YS**PL) (7,19)

(Fig. 1). Under basal conditions, Ser650 is constitutively phosphorylated, and as a result lipid kinase activity and talin binding are suppressed. Integrin signaling via FAK and Src promotes Tyr649 phosphorylation, either directly (19) or indirectly by suppressing phosphorylation of the adjacent Ser650 (7). Tyr649 phosphorylation promotes interaction with talin and stimulates lipid kinase activity (19). The model that emerges is that integrin signaling increases PIP_2 synthesis at FA by recruiting and activating PIP5Kγ90, and the localized increase in PIP_2 activates talin, which then binds and further activates integrins. The signal is turned off by PIP5Kγ90 dephosphorylation, and Shp-1 Tyr phosphatase, which has been previously implicated in the regulation of FA dynamics, dephosphorylates PIP5Kγ90 (5). FA turnover is therefore dynamically regulated via the reciprocal actions of multiple FA components by Src and Shp-1.

More recently, the same group has shown that epidermal growth factor (EGF) receptor directly phosphorylates Tyr649 (Fig. 1) and that this event is required for cell migration after EGF stimulation (4). Tyr649 phosphorylation also regulates PIP5Kγ90 interaction with PLCγ. Unphosphoyrlated PIP5Kγ90 associates with PLCγ, while tyrosine phosphorylated PIP5Kγ90 dissociates with PLCγ and binds to talin to mediate the cell migration induced by EGF.

Unlike PIP5Kγ90, PIP5Kγ87 is not found in FA and does not bind talin (18,19). Nevertheless, it has also been implicated in integrin adhesion via a PLD2-mediated, but actin-independent, mechanism (128). PIP5Kβ overexpression has no effect on spreading. These results raise the possibility that PIP5Kγ90 and 87 may be involved in different stages of FA formation or turnover, while PIP5Kβ is not.

Synaptic vesicle physiology

The PIP_2 level is increased in neurons in response to K^+-induced depolarization (17), and it regulates synaptic transmission by multiple mechanisms. PIP_2 is the immediate precursor of PLC-generated $InsP_3$ and DAG, which activate Ca^{2+} signaling and PKC, respectively. PIP_2 also directly regulates exocytosis and endocytosis by binding to clathrin adaptors and other endocytic proteins, by priming exocytic vesicle, by promoting membrane fusion and fission, and by regulating the actin cytoskeleton. Synaptojanin, which dephosphorylates PIP_2, is also required for normal synaptic vesicle cycling and actin dynamics at the synapse (166).

PIP5Kγ90 overexpression in chromaffin cells increases the amount of PM PIP_2 as well as the number of vesicles in the docked releasable pool (78). The importance of PIP5Kγ in vesicle trafficking is confirmed by gene knockout. Synaptosomes prepared from the brains of the *PIP5Kγ-/-* mice have 40% less PIP_2 than WT, and they do not generate PIP_2 in response to K^+ depolarization. Although primary cultures of cortical neurons develop normally *in vitro* in spite of the lack of PIP5Kγ, they have severe defects in synaptic transmission, which correlate with abnormal exocytosis and clathrin-mediated endocytosis (17). Likewise, chromaffin cells isolated from these mice have defective vesicle priming and fusion dynamics (158).

In another *PIP5Kγ-/-* mouse model, knockout mice exhibited neural tube closure defects that were associated with impaired PIP_2 production, adhesion junction formation, and neuronal cell migration (20). Consistently, megakaryocytes isolated from *PIP5Kγ-/-*

mice have membrane blebbing accompanied by a decreased association of the membrane with the cytoskeleton, probably through a pathway involving talin (24).

Recently, a mutation (D253N) has been mapped in PIP5Kγ gene in human Lethal Contractural Syndrome type 3 patients (167). This point mutation abrogates the lipid kinase activity of PIP5Kγ which leads to the decrease of PIP_2 synthesis and culminates in lethal congenital arthrogryposis.

Talin, which regulates PIP5Kγ90 in FA, is also present in synapses. Disruption of talin:PIP5Kγ90 interaction induces actin depolymerization and decreases clathrin-mediated synaptic vesicle endocytosis (168). These results suggest that PIP5Kγ90 is regulated by talin in neurons using mechanisms similar to those in FAs. Likewise, neuronal PIP5Kγ90 is also reciprocally regulated by Ser and Tyr phosphorylation. In neurons, PIP5Kγ90 is constitutively phosphorylated on Ser650 by p35/Cdk5 and MAPKs, and it is dephosphorylated during K^+-induced depolarization by calcineurin (137,160). Ser650 dephosphorylation activates PIP5Kγ90 and facilitates Tyr649 phosphorylation by Src. Significantly, K^+-induced depolarization also promotes PIP5Kγ90 interaction with Arf6, which would further promote PIP_2 synthesis (104,154). Thus, PIP5Kγ is activated through a confluence of different and interrelated signals during neuronal stimulation.

Interaction with clathrin adaptor protein complexes

The clathrin adaptor protein complex AP-2 is activated by PIP_2 to bind its transport cargoes at the PM (169). Now there is evidence that AP-2 directly participates

in increasing PIP_2 synthesis at the nascent endocytic site by binding and activating PIP5Ks. Therefore it is attractive to hypothesize that the coincidence detection of membrane cargoes and PIP_2 by AP-2, together with AP-2 activation of PIP5Ks, specify the site-specific generation of a local PIP_2 pool that is dedicated to clathrin/AP-2 dependent endocytosis (34).

The details of how this occurs remain to be explored. One study reports that the μ subunit of AP-2 binds all PIP5Ks (170). Thus, AP-2 binding to PIP5Kβ may explain how PIP5Kβ promotes endocytosis in HeLa cells (21) (see above). However, other studies show that the interaction with AP-2 is mediated primarily through the PIP5Kγ90 tail, which is not present in the other PIP5Ks. Tail binding to AP-2 potently stimulates PIP5Kγ90's lipid kinase activity (6,145). Overexpression of the PIP5Kγ90 tail, which competes with endogenous PIP5Kγ90 for AP-2, decreases AP-2 recruitment and synaptic vesicle endocytosis (6). The trafficking abnormalities are similar to those described in *PIP5K*γ-/- neurons (17), suggesting that PIP5Kγ90 binding to AP-2 is physiologically relevant, and that the neuronal defects in *PIP5K*γ-/- mice can be attributed at least partly to the lack of PIP5Kγ90.

PIP5Kγ has been implicated in membrane trafficking in nonneuronal cells as well. Overexpression of WT PIP5Kγ90 in MDCK cells increases transferrin uptake, while overexpression of KD PIP5Kγ90 inhibits (145). These effects are specific for the long splice variant of PIP5Kγ, because PIP5Kγ87 overexpression has little effect (145).

Recently, the PIP5Kγ90 tail has been reported to bind to another clathrin adaptor AP-1 (6,131). This interaction is proposed to be critical for E-cadherin trafficking and

adhesion junction formation (131). Since AP-1 is located primarily at the TGN, and it binds PI(4)P instead of PIP_2 (27,171), this interaction is perplexing. Furthermore, PIP5Kγ87, which does not have the tail, has also been implicated in cadherin and actin enriched cell:cell adhesion in the epithelial A431 cells (172). PIP5Kγ has also been shown to be recruited by N-cadherin to locally generate PIP_2 (173). The PIP5Kγ-generated PIP_2 pool is critical for the formation and strength regulation of the intercellular adhesion partially through its regulation of gelsolin.

$InsP_3$-mediated Ca^{2+} signaling

PIP_2 is critical to intracellular Ca^{2+} signaling, because it is the obligatory precursor of $InsP_3$. RNAi studies show that although depletion of both PIP5Kγ90 and 87 isoforms together (using siRNA directed against a common sequence) decreases total PIP_2 by less than 15% in HeLa cells, it blocks histamine induced, heterotrimeric G protein activated $InsP_3$ generation by more than 70% (16). Ca^{2+} flux is also inhibited. However, depletion of PIP5Kγ90 with the unique tail specific siRNA has no effect. Therefore, these results suggest that PIP5Kγ87 is important for G protein-coupled receptor signaling. Remarkably, depletion of PIP5Kβ or α, which individually accounts for a larger fraction of total PIP_2 than PIP5Kγ in HeLa cells, has almost no effect on $InsP_3$ generation. Single cell immunofluorescence imaging shows that the PIP5Kγ and PIP5Kβ depleted HeLa cells have a similar drop in PM PIP_2, but that the latter has more PIP_2 loss in internal membranes as well. The exquisitely selective effect of PIP5Kγ87 depletion on

Ca^{2+} signaling suggests that the PM PIP_2 pools generated by PIP5Kγ87 and β are functionally compartmentalized (16).

This finding again raises the important question of how the PIP_2 pools existing on the same PM can have distinct functions. One possibility is that if PIP5Kγ87 is part of a supramolecular PLCβ signaling scaffold that specifies rapid local Ca^{2+} generation and propagation (174), while PIP5Kβ is not. In this model, the PIP_2 generated by PIP5Kγ87 would be immediately available for hydrolysis by PLCβ within the signaling scaffold, thus behaving like the previously proposed agonist-sensitive, *de novo* synthesized PIP_2 pool (175,176). In contrast, the PIP_2 generated by PIP5Kβ may represent a preexisting agonist-insensitive pool that maintains the PM's *status quo*. The two PIP_2 pools may physically segregated from the other PIP_2 pool by interaction with scaffolding proteins. Studies using heart sarcolemma support the existence of agonist sensitive and insensitive PIP_2 pools (74,84).

A similar approach, depleting individual PIP5K isoform by shRNA, in natural killer cells revealed that both PIP5Kγ and α-generated PIP_2 pools are required for $InsP_3$ production and lytic granule exocytosis induced by receptor stimulation while they are redundant in the control of PI3K activation and granule polarization (22). Moreover, platelets from *PIP5K*α-/- (mouse *PIP5K*β-/-) mice showed severe decrease in $InsP_3$ generation after thrombin stimulation (23). PIP5Kα and β double knockout completely abolished the $InsP_3$ signaling even thought these platelets still have a normal amount of PIP5Kγ. All of these suggest that compartmentalized PIP_2 pools maintained by PIP5K isoforms could be functionally different in a tissue or cell type-depedent manner.

Mammalian PIP5Kα

PIP5Kα is ubiquitously expressed (94,95) and found in multiple cell compartments. Like other PIP5Ks, it is partly cytosolic and partly PM associated. However, PIP5Kα is also found in the nucleus (108). The *PIP5Kα*-/- (mouse *PIP5Kβ*-/-) mice have recently been made and their birth rate occurs at a slightly less than anticipated frequency (23). Those who survived to birth appeared normal and survived to adulthood but produced few offspring. The *PIP5Kα*-/- platelets exhibited abnormal aggregation as well as disaggregation. They also had impaired $InsP_3$ formation and PIP_2 synthesis defects after thrombin stimulation (see below).

Membrane ruffling

The PM ruffles in response to many types of stimuli, and requires remodeling of cortical actin networks downstream of the activation of Rac (177). PIP_2 has long been implicated in this process, because Rac and Arf6 regulate PIP5Ks and induce ruffling. In MG-63 fibroblasts, PIP5Kα, but not β, translocates to the PM after PDGF stimulation (138). Overexpressed PIP5Kα promotes the formation of actin foci formation when Rac1 is inhibited, but stimulates ruffle formation when Rac1 is activated. These results suggest that PIP5Kα promotes actin assembly, and that additional inputs from Rac1 are required to generate active ruffles. The LIM protein ajuba, which is a component of the integrin-mediated adhesive complex and a Rac activator, is a potential effector (112). It promotes PIP5Kα localization to membrane ruffles and leading lamellipodia.

B cell and platelet activation

Upon the engagement of B cell receptors (BCRs), PIP5Kα is recruited to the PM by Bruton's Tyr kinase which has a PH domain (81). Membrane fractionation shows that PIP5Kα is translocated to lipid rafts, where PIP_2 is converted to second messengers including PIP_3, $InsP_3$ and DAG.

Phagocytosis

Actin remodeling during FcγR-mediated phagocytosis is regulated by a highly orchestrated series of events (11,26). One of the initial changes is a localized increase in PIP_2 at the nascent phagocytic cup. PIP5Kα is recruited to the phagocytic cup, and overexpression of a PIP5Kα KD mutant blocks actin remodeling and PIP_2 accumulation there (11,26). PIP5Kβ has been implicated in integrin-mediated *Yersinia* phagocytosis (134). The PIP_2 increase is critical for actin modeling at the phagocytic cup. PIP_2 promotes actin assembly by recruiting WASP family proteins to induce Arp2/3 dependent actin nucleation, and PIP_2 also inhibits gelsolin to prevent actin severing during the ingestion phase (178).

Receptor-mediated endocytosis

Like PIP5Kβ and γ, PIP5Kα has also been implicated in receptor-mediated endocytosis. Overexpression of a PIP5Kα truncation mutant (Table 2), which has little kinase activity and is not recruited to the PM, inhibits the endocytosis of EGFR (130) and

mutated colony stimulating factor (CSF)-1 receptor which is endocytosed more rapidly (139).

$InsP_3$ signaling

The *PIP5K*α-/- platelets had striking deficiency in PIP_2 synthesis and $InsP_3$ formation after thrombin stimulation, suggesting that after stimulation of G protein-coupled receptor $InsP_3$ is derived from the rapidly replenished discrete PIP_2 pool partially synthesized by PIP5Kα (23). Thrombin activation of platelets induces recruitment of PIP5Kα to the PM in a Rho and ROCK-mediated, but Rac1-independent, manner (80). The recrtuiment of PIP5Kα could be directly mediated by β-arrestins. Following the stimulation of β2 adrenergic receptor, β-arrestins act as scaffolding proteins to interact with PIP5Kα and the receptor to form a signaling complex (179). Locally synthesized PIP_2 is required for the recruitment of more β-arrestins to amplify the signaling cascade and AP-2 complex to initiate the receptor internalization essential for the termination of the signal. PIP5Kα has also been shown to be recruited by E-cadherin-catenin complex to the PM after extracellular Ca^{2+} treatment in keratinocytes (180). The recruitment is critical for the activation of PIP5Kα and the generation of PIP_2 which provides substrate for PI3K and PLCγ and is important for their downstream signaling pathways including Akt phosphorylation, $InsP_3$ production, and eventually the keratinocyte differentiation.

Apoptosis

PIP5Kα, but not PIP5Kβ or γ, is cleaved by caspase 3 during apoptosis, and overexpression of PIP5Kα protects cells against apoptosis by inhibiting caspase activity (39). Protection is dependent on PIP_2 generation, because KD PIP5Kα shows no protection. The mechanism of protection is however different from that ascribed to PIP5Kβ, which is not cleaved by caspase 3 and which prevents upstream of caspase activation (40).

Cytokinesis

PIP_2 enrichment has been detected in the cleavage furrow and it is required for the completion of cytokinesis (181). During cytokinesis, RhoA recruits PIP5Kα (and β, but not γ) to the cleavage furrow and overexpression of KD PIP5Kα blocks the PIP_2 accumulation therefore compromise cytokinesis. Interference of PIP_2 impairs the adhesion of the PM to the contractile ring at the furrow suggesting at least the partial role PIP_2 plays during cytokinesis (182).

Nuclear PIP_2

There is increasing evidence that the nucleus has its own phosphatidylinositol machinery (183). PIP_2 is found in nuclear speckles, which contain mRNA-processing components that are used for chromatin remodeling (108). The PDZ domain-containing protein syntenin-2 is targeted to the nuclear speckles by binding PIP_2, and syntenin-2 depletion by RNAi disrupts PIP_2 nuclear speckles, and impairs cell survival (184). Nuclear PIP_2 has also been implicated in mRNA processing, transcriptional regulation,

cell cycle regulation and stress responses (183,185,186). PIP5Kα and PIP4K, which synthesize PIP_2 using different routes, are both found in the nucleus, and type III PI4Kα, which generates the PIP5K substrate PI(4)P has been identified there as well (187). PIP5Kα does not have a recognizable nuclear localization signal. However, its C-terminal extension is required for PIP5Kα binding with a polyA polymerase, StarPAP which is localized in the nucleus. This interaction could be critical since this region is sufficient and necessary for nuclear targeting of PIP5Kα (188). But the molecular mechanism for its shuttling between the nucleus and cytoplasm remains to be identified. The *S. cerevisiae* and *Drosophila* PIP5Ks are also partially nuclear localized, and they have a nuclear localizing signal (121,189).

PHAGOCYTOSIS

Phagocytosis, a critically important component of innate host defense, inflammation and tissue remodeling, is the mechanism by which cells internalize large particles (>0.5 μm) by various phagocytic receptors present on their surface (8,10). Among those, the best understood and the most extensively studied are FcγRs, which are expressed in nearly all haematopoietic cells and are involved in the recognition and uptake of immunoglobulin G (IgG)-opsonized pathogen and immune complex (IC) during infection (9,190). FcγR-mediated phagocytosis consists of a series of spatially and temporally regulated events including particle attachment, engulfment, and phagosome maturation (8,10).

FcγR microclustering

Upon interaction with IgG, FcγRs are induced to laterally assemble ("cluster") within the PM (191). The microclustering of FcγRs, which have comparatively low affinity, is essential for their stable interaction with multivalent ligands therefore efficiencient particle attachment (192). In addition, it initiates several signaling cascades starting with the activation of Src kinases (9). Src kinases phosphorylate an immunoreceptor tyrosine-based activation motif (ITAM) domain located in the cytoplasmic side of FcγR. ITAM tyrosine phosphorylation mediates the recruitment and auto-activation of Syk kinase which facilitates FcγR clustering in a positive feedforward manner . Other downstream signaling events include the PLCγ1 phosphorylation leading to PKC activation and calcium mobilization, the recruitment and activation of guanine

nucleotide exchange factors (GEFs) for Rho GTPases Rac and Cdc42, and the activation of Ras pathway such as extracellular signal-regulated kinase (ERK). The clustering of other ITAM containing receptors such as T cell receptor (TCR) and BCR has also been shown to be important for their effective and sustained activation (193,194). The actin cytoskeleton and its regulators have been demonstrated to be essential to drive and maintain the formation of TCR or BCR microclusters (195,196). However, the role of the actin cytoskeleton in FcγR clustering remains largely unknown.

Actin, PIP_2, and PIP5Ks dynamics during phagocytosis

Once a particle has bound, transient and localized actin polymerization is required for particle engulfment (197). Actin assembles at the nascent phagocytic cup and disassembles during the completion of internalization. In parallel to actin dynamics, the PIP_2 level increases focally in the cup during ingestion and decreases prior to engulfment (11). Overexpression of DN PIP5Kα inhibits pseudopod extension while overexpression of WT PIP5Ks or pharmacological inhibition of PLCγ blocks the sealing of the phagocytic cup to form a phagosome (26,59). Thus, PIP_2 synthesis promotes *de novo* actin polymerization to initiate particle ingestion while PIP_2 dissipation depolymerizes actin to promote the termination of engulfment. Since all three PIP5K isoforms are recruited to the phagocytic cup with similar dynamics (59), the contribution of which PIP5K isoform to the localized PIP_2 increase during particle ingestion is still undefined.

CHAPTER THREE
Methodology

ANTIBODIES, CDNA CONSTRUCTS AND REAGENTS

All chemicals and reagents were obtained from Sigma-Aldrich unless indicated otherwise. Other materials: recombinant CSF-1 (R&D Systems); polyclonal anti-PIP5Kγpan and -PIP5Kγ90 (160); anti-PIP5Kβ (Gift from CL Carpenter, Harvard Medical School, Boston, MA) (80); anti-PIP5Kα, -RhoA, -ERK, -Syk, -myc, -WASP and -phosphotyrosine (pY) (Santa Cruz Biotechnology); anti-active WASP (Gift from MK Rosen, UT Southwestern, Dallas, TX) (198); anti-Rac1, -N-WASP and -p34-Arc (Upstate Biotechnology); PE-anti-CD45.1, FITC-anti-CD45.2, APC-anti-CD4, and anti-FcγRIIB/III mAb 2.4G2 (BD Biosciences); anti-pERK (Cell Signaling); anti-actin (Chemicon); fluorescent-conjugated secondary antibodies (Jackson ImmunoResearch Laboratories); HRP-conjugated secondary antibodies (Amershan Biosciences); ^{32}P-PO_4 and [γ-^{32}P]ATP (PerkinElmer); C3 transferase (C3T) (Cytoskeleton Inc.); Jasplakinolide (Jasp.) and piceatannol (Calbiochem); Latr. B (Molecular Probes). Epitope tagged PIP5Ks were as described previously (21). Human Syk and DN Syk (Syk SH2 domain only, aa 1-261) were cloned into the pCMV5 vector (199).

BONE MARROW TRANSPLANTATION AND BMM DIFFERENTIATION *IN VITRO*

PIP5Kγ-/- mice were generated by breeding *PIP5Kγ*+/- mice (17). Liver cells isolated from newborn *PIP5Kγ*-/- or +/+ pups (C57BL/6J CD45.2) were injected into lethally irradiated WT adult recipient mice (C57BL/6J CD45.1). The genotypes of the newborn donor mice used for transplantation were established by PCR analysis of genomic DNA isolated from mouse heads. Reconstitution in the chimera was confirmed by FACs analysis. Bone marrow progenitor cells were isolated 3 to 9 months post transplantation. *PIP5Kα*-/- mice (human isoform designation, even when referring to knockout in mice) were generated by breeding *PIP5Kα*+/- mice (23) and used directly for bone marrow isolation. *PIP5Kα*+/+ mice from the same litter were used as WT controls. Bone marrow progenitor cells were cultured in macrophage differentiation medium [DMEM containing 30% L929-conditional medium, 1% (v/v) MEM vitamins and 1% (v/v) penicillin/streptomycin] (200) and used for experiments after 5 to 10 days in culture.

BMM RESPONSE TO CSF-1

BMM were serum starved overnight and stimulated with 30 ng/ml of CSF-1. Cells were either processed for fluorescence microscopy after staining with TRITC-phalloidin or subjected to Western blotting using antibodies against total ERK and phosphorylated ERK. The average number of ruffles per cell was expressed as a ruffle index.

FLOW CYTOMETRY

To determine reconstitution efficiency

Spleen cells collected from chimeric mice were simultaneously stained with PE-anti-CD45.1, FITC-anti-CD45.2 and APC-anti-CD4 and sorted by FACSCalibur (BD Biosciences). CD4+ cells were gated and their CD45.1/CD45.2 profiles were determined.

To determine the amount of FcγR on the BMM cell surface

BMM were fixed and suspended at 2.5×10^7 cells/ml in PBS containing 3% BSA. Cells were incubated with 2.4G2 (1:50) at RT for 60 min, stained with Alex488-conjugated goat anti-rat IgG (1:200) for 30 min at RT and subjected to FACScan analysis. Autofluorescence was determined in cells without 2.4G2 staining. Data were analyzed using the CellQuest software (BD Biosciences).

QUANTITATIVE RT-PCR

Total RNA was extracted and reverse transcribed to generate cDNA for PCR in an ABI Prism 7000 sequence detection system (Applied Biosystems). The mRNA level of PIP5K was determined by comparing its mean threshold cycle to that of cyclophilin. Primers used: cyclophilin: forward: 5'-TGGAGAGCACCAAGACAGACA-3' and reverse: 5'-TGCCGGAGTCGACAATGAT-3'; PIP5Kα: forward: 5'-AGAAGTTGGAGCACTCTTGG-3' and reverse: 5'-GAGAAGGCTTCAAGGGAATC-

3'; PIP5Kβ: forward: 5'-AGGAGATCGTATCCTCCATC-3' and reverse: 5'-AATGATGGAGTGCTGGGTAC-3'; PIP5Kγpan: forward: 5'-TGTTGCCTTCCGCTACTTC-3' and reverse: 5'-GGCTCATTGCACAGGGAGTAC-3'; PIP5Kγ90: forward: 5'-AGCCTCTGTGGAAATAGACGCT-3' and reverse: 5'-GAGTACACCCAGCTCCTCTCGT-3'.

IMMUNOFLUORESCENCE MICROSCOPY

For most experiments, cells were fixed with 3.7% formaldehyde, permeabilized with 0.1% Triton X-100 and processed for confocal microscopy. In some cases, cells were fixed but not permeabilized prior to staining to detect epitopes on the cell surface. Images were collected by a 63×/NA 1.4 Plan Apo oil-immersion objective (Carl Zeiss) on a laser scanning confocal microscope Axiovert 100M (Carl Zeiss) using LSM 510 Meta software (Carl Zeiss).

PHOSPHOINOSITIDE MEASUREMENTS

Thin layer chromatograph

^{32}P incorporation into PIP and PIP_2 was determined by labeling cells for 4 h with 35 μCi/ml ^{32}P-PO_4 in phosphate-free DMEM (Invitrogen) (101). Lipids were extracted, resolved by thin layer chromatograph (TLC), detected by autoradiography and analyzed

by ImageQuant TL software (GE Healthcare). The amount of ^{32}P-PIP_2 or PIP was expressed as a percent of ^{32}P incorporation into total phospholipids in the autoradiogram.

High presseur liquid chromatograph

Lipid mass was determined and normalized against total lipids eluted as described previously (132). Briefly, phospholipids were extracted from 10-cm dish of BMM, deacylated and subjected to anion-exchange high presseur liquid chromatograph (HPLC) in an Ionpac AS11 colomun. Negatively charged glycerol head groups were eluted with a 10 to 80 mM NaOH gradient and detected by suppressed conductivity in a Dionex AS50 system equipped with an ASRS-ultra self-regenerating suppressor.

PHAGOCYTOSIS ASSAYS

Latex beads

Latex particles were opsonized with 1 mg/ml human IgG (1 h at 37ºC or overnight at 4ºC) (26). In most cases, 3 μm beads were used, except for Fig. 18, in which 1 μm beads were used to increase the extent of stimulation for phosphorylation experiments. Particles in serum-free medium were allowed to attach to cells for 10-15 min at 4ºC and washed extensively (binding). For ingestion, cells were incubated in serum-free medium for 5 min (for BMM, unless otherwise indicated) or 15 min (for CHO-IIA cells, unless otherwise indicated) at 37ºC. Externally accessible beads were detected by labeling fixed but not permeabilized cells with anti-human IgG for 10 min. Proteins inside cells were stained after permeabilization of the fixed cells. Differential

interference contrast (DIC) microscopy was used to visualize beads (external and internal) and confocal laser microscopy was used to visualize fluorescently labeled proteins. The number of beads on the cell surface or inside the cells was counted in 5-10 randomly chosen fields (with approximately 30-50 cells per field) and expressed as the binding or ingestion index (mean number of beads/cell), respectively.

Sheep red blood cells

Formaldehyde-fixed sheep red blood cells (SRBC) (ICN/Cappel, Durham, NC) were opsonized with either rabbit anti-sheep IgG (1:5000, ICN) or IgM (1:1000, Accurate Scientific, Westbury, NY) at 37ºC for 1 h in gelatin veronal buffer. The IgM-opsonized SRBC were further incubated for 20 min at 37ºC with 10% C5-deficient serum to acquire C3bi. Opsonized SRBC were washed, resuspended and added to BMM (SRBC/BMM ratio 10). BMM used for complement-mediated phagocytosis were pretreated with 100 ng/ml PMA (Calbiochem, San Diego, CA) for 15 min to activate the C3R. Ingested SRBC were identified after hypotonic lysis of external SRBC (30 sec at 4ºC in water). Cells were fixed, permeabilized and stained with FITC-conjugated phalloidin and TRITC-conjugated anti-rabbit IgG or IgM. Attached or ingested SRBC were quantitated as described above.

IC-INDUCED FCγR CLUSTERING

FcγR clustering assay by using IC was performed as previously described (191). Briefly, 10 mg/ml human IgG (Sigma) was heated for 25 min at 63ºC, cooled on ice, and

centrifuged to clarify large aggregates of IgG. The supernatant containing IC was diluted by serum free medium (100 μg/ml final) and applied to CHO-IIA cells or BMM plated on 12-mm glass coverslips for 5 and 20 min at 4ºC. Cells were washed with PBS to remove unbound IC, fixed and permeabilized. IC-induced clusters were visualized by either staining of IC with FITC-conjugated anti-human IgG or staining of FcγR by 2.4G2 followed by Alexa488-conjugated anti-rat IgG antibody. Fluorescent images were taken with a confocal laser microscopy system (Carl Zeiss LSM510) at the same settings and the size of the clusters (expressed as square pixels) was analyzed with ImageJ software and calibrated as arbitrary unit. At least 20 cells from two independent experiments were analyzed in each variant, and 40 to 50 clusters were scored in every cell. For analysis of ERK activation by binding of IC, the cells were suspended, challenged with IC at 4ºC for 20 min, washed, and incubated at 37ºC for the time indicated, lysed with regular RIPA buffer, subjected to SDS-PAGE and immunoblotted using antibodies against total ERK and phosphorylated ERK1/2.

FLUOROMETRIC PHALLOIDIN ACTIN QUANTITATION

Phalloidin binding to fixed and permeabilized BMM was quantitated fluorometrically (201). BMM attached to a 24-well plate were fixed, permeabilized and stained with FITC-phalloidin (0.35 μM) and DAPI (10 μg/ml). Samples were excited at 360/480 nm and emissions at 460/530 nm were recorded by FL600 microplate fluorescence reader (Bio-Tek). F-actin content per cell was defined as the ratio of FITC to DAPI fluorescence intensity, after subtracting background autofluorescence.

PIP_2 SHUTTLING

Carrier 3 and diC16-PIP_2 (both from Echelon Biosciences) were premixed at equal molar ratio (each at 100 μM) at RT for 10 min and added to BMM at a final concentration of 10 μM (27). After 10 min incubation at 37ºC, the medium was replaced with serum-free medium containing particles for binding assays. Control cells were incubated with shuttle carrier without PIP_2.

GTP-RAC AND -RHO EFFECTOR PULL DOWN ASSAYS

BMM were lysed in a buffer containing 25 mM HEPES, pH 7.5, 150 mM NaCl, 10 mM $MgCl_2$, 1 mM EDTA, 10% glycerol, 1% NP-40 and protease inhibitors. Clarified lysates were incubated with either GST-PAK-PBD or GST-Rhotekin-RBD immobilized on glutathione-Sepharose 4B beads (Cytoskeleton Inc.) for 45 min at 4ºC. Rac1 and RhoA contents were determined by Western blot.

TAT-RAC1 PROTEIN TRANSDUCTION

The HA-tagged Tat-Rac1L61 (CA) and Tat-Rac1N17 (DN) constructs were gifts of C. Wulfing (UT Southwestern, Dallas, TX). Recombinant Tat-fusion proteins were expressed in BL21(DE3) bacteria (Novagen) and purified under non-reducing conditions (202). Purity of the proteins was about 95% as determined by SDS-PAGE and

subsequent Coomassie blue staining. Protein expression was confirmed by immunoblotting using anti-HA and anti-Rac1 antibodies. Suspended BMM (2×10^6 cells/mL) were incubated with 600 nM Tat-Rac1 for 30 minutes at 37°C in polyhema-coated 6-well plate. After incubation, cells were harvested, washed, and either lysed or seeded onto coverslips. Cell lysates were subjected to SDS-PAGE and immunoblotted with anti-HA and anti-Rac1 antibodies. After 10 min, the attached cells were fixed, permeabilized, and stained with anti-HA antibody followed by FITC-conjugated secondary antibody. Uptake of Tat-Rac1 proteins were confirmed by both Western blot and immunofluorescence. The attached cells after 10 min were challenged with IgG-opsonized particles in a phagocytosis assay or were stained with phalloidin and DAPI to measure the F-actin.

RNA INTERFERENCE

CHO-IIA cells (Gift from S Grinstein, Hospital for Sick Children, Toronto, ON, Canada) that stably expressed human FcγRIIA were maintained in DMEM containing 10% FBS and 0.5 mg/ml G418. They were seeded at a density of 5×10^4 cells/12-mm glass coverslip and transfected with siRNA using Oligofectamine (Invitrogen). Cells were used 48 h later. Hamster PIP5K sequences were obtained by cloning using primers from conserved human/mouse sequences (PIP5Kα: forward: 5'-GCTGCAGAGCTTCAAGAT-3' and reverse: 5'-GAACTCTGACTCTGCAAC-3'; PIP5Kγ: forward: 5'-AAGCCACCACAGCCTCCAT-3' and reverse: 5'-

TTATGTGTCGCTCTCGCC-3'. The siRNA used were 5'-AAATCAGTGAAGGCTCACCTG-3' and 5'-ATCATCAAGACCGTCATGCAC-3' for PIP5Kα and γ, respectively. An oligonucleotide (5'-AAGAATATTGTTGCAC-3') that targets firefly luciferase was used as a control.

IN VITRO PIP5K PHOSPHORYLATION BY SYK

COS cells were separately transfected with myc-PIP5K and Syk using Lipofectamine 2000 (Invitrogen). Cells were lysed and myc-PIP5K or Syk was immunoprecipitated with anti-myc or -Syk and protein G-Sepharose beads. Beads were resuspended in kinase buffer (50 mM Hepes, pH 7.4, 10 mM $MgCl_2$, 10 mM $MnCl_2$ and 10 μM sodium vanadate) in the presence or absence of piceatannol. ATP was added to a final concentration of 2 μM and *in vitro* phosphorylation was terminated after 20 min at RT. Tyrosine phosphorylation was detected by Western blot with anti-pY.

IN VITRO LIPID KINASE ASSAY

COS cells were transfected with myc-PIP5Kγ87. 24 h later, cells were treated for 10 min with or without 2 mM PV freshly prepared from orthovanadate and hydrogen peroxide (107). Myc-PIP5Kγ87 was immunoprecipitated with anti-myc/protein G Sepharose beads. The beads were suspended in a solution containing 50 mM Tris-HCl, pH 7.4, 100 mM NaCl, 15 mM $MgCl_2$, 1 mM EGTA, 0.4 mg/ml BSA, 250 mM sucrose,

0.4% PEG 20,000, 0.04% Triton X-100, and 80 μM PI4P and 80 μM phosphatidylserine (Avanti Polar Lipid) (132). [γ-^{32}P]ATP was added (1 μCi/50 μl, 50 μM final) and phosphorylation was terminated after 10 min at RT. Lipids were separated by TLC and quantified by Phosphorimager (GE Healthcare) analysis. Equivalent immunoprecipitates were Western blotted by anti-myc and -pY. Specific lipid kinase activity was obtained by normalizing ^{32}P-PIP_2 to the amount of immunoprecipitated myc-PIP5Kγ87 as determined by Western blot.

STATISTICAL ANALYSIS

All data were expressed as mean±SEM, and the two-tailed unpaired *t*-test was used to analyze the statistical significance.

CHAPTER FOUR
Results

BMM HAVE PIP5Kα AND ABUNDANT PIP5Kγ87

Western blot was used to compare the expression level of PIP5Ks in BMM with other types of cells. BMM had abundant PIP5Kγ, some PIP5Kα and almost no detectible PIP5Kβ (Fig. 2). The RAW264.7 macrophage-like cell line and non-myeloid COS cells also had abundant PIP5Kγ, and more PIP5Kα and β than BMM. In contrast, HeLa and CHO-IIA cells had more PIP5Kα and less PIP5Kβ and γ. I did not detect the γ90 variant in BMM even though it should be recognized by the anti-PIP5Kγpan antibody used (160). PIP5Kγ90's low abundance was confirmed by lack of staining with another antibody directed against PIP5Kγ90's unique COOH-terminal extension (data not shown) (160).

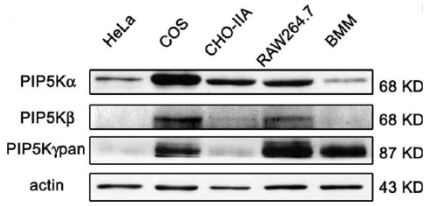

Figure 2. Western blot of endogenous proteins in WT BMM.

Quantitative RT-PCR showed that PIP5Kγ87 was most abundant at the mRNA level in BMM compared with the other isoforms (Fig. 3), corroborating the Western blot results. PIP5Kγ90 and β mRNA were about 4% and 1% of PIP5Kγ87, respectively. In this dissertation, I will use gene knockout and RNAi to examine the roles of PIP5Kγ and α during FcγR-mediated phagocytosis.

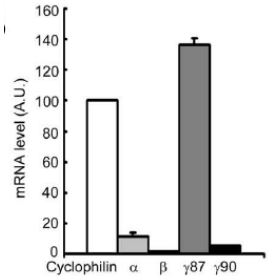

Figure 3. Quantitative RT-PCR. PIP5K level in WT BMM was normalized against cyclophilin (n=3).

*PIP5K*γ-/- BONE MARROW PRECURSOR CELLS DIFFERENTIATE INTO BMM

Immunofluorescence labeling with anti-PIP5Kγpan showed that PIP5Kγ, which was predominantly cytosolic, was recruited to the nascent phagocytic cup during FcγR-mediated phagocytosis (Fig. 4A). I used PIP5Kγ knockout to examine its role in BMM. Since *PIP5K*γ-/- mice die within a day of birth (17), their hematopoietic precursor cells were transplanted into lethally irradiated WT adult mice to generate sufficient *PIP5K*γ-/- cells for experimentation. *PIP5K*γ+/+ cells from pups from the same litter were transplanted in parallel to generate matched *PIP5K*γ+/+ chimeras (WT controls). Reconstitution in the chimeras was established by flow cytometry to be 86 to 99% (Fig. 4B). Western blot confirmed that the *PIP5K*γ-/- chimeric mice's BMM had no detectible PIP5Kγ (Fig. 4C). Nevertheless, they expressed normal amount of FcγR as assayed by Western blot with the 2.4G2 antibody that detects type II and III receptors (Fig. 4C) and by FACs analyses of externally labeled FcγR (Fig. 4D). In addition, like

WT BMM (203), *PIP5K*γ-/- BMM responded to CSF-1, a major macrophage growth and chemotactic factor, by robustly activating ERK (Fig. 4E) and ruffling their PM (Fig. 13B). Therefore, they are *bona fide* macrophages.

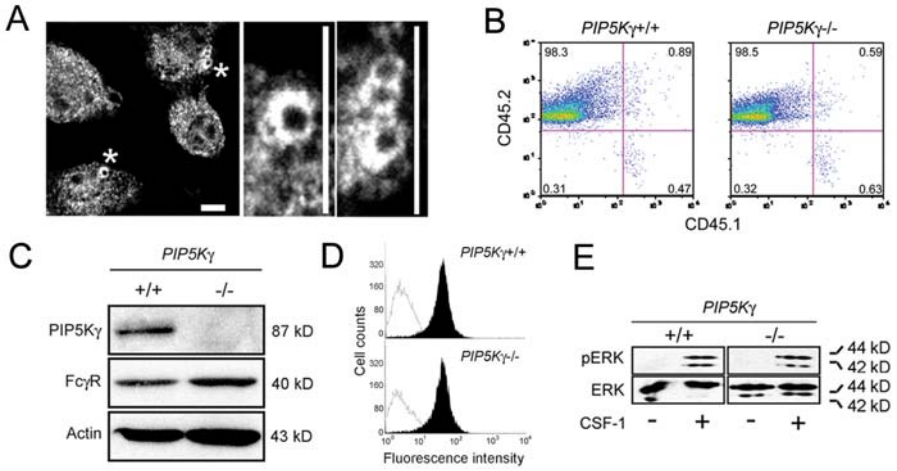

Figure 4. Characterization of *PIP5K*γ in BMM. (A) Recruitment of PIP5Kγ to the phagocytic cup. WT BMM exposed to IgG-opsonized particles were stained with anti-PIP5Kγpan antibody. The middle and right panels show zoomed in views of regions marked by asterisks. Scale bars in all figures, 10 μm. (B) The extent of reconstitution of CD45.2 donor cells in CD45.1 recipient chimeric mice was assayed by FACs. Spleen cells isolated from chimeric recipient mice were analyzed after staining with anti-CD45.2, -CD45.1 and -CD4 antibodies. The % of CD4+ cells positive for each genotype marker was indicated in the corner of each quadrant. (C) Western blot of *PIP5K*γ-/- BMM. (D) FACs analysis of surface accessible FcγR. Black peaks, surface FcγR fluorescence; white peak, background. (E) CSF-1-induced ERK activation. CSF-1 stimulated BMM were extracted for Western blot with anti-ERK and -pERK.

Although WT BMM have abundant PIP5Kγ, PIP5Kγ knockout had surprisingly little effect on ambient PIP_2 content, as assessed by TLC, which depends on PIP_2 turnover, and by HPLC, which measures lipid mass (Fig. 5A). Western blot did not detect a significant compensatory increase in PIP5Kα in BMM (Fig. 5B), concurring with results from *PIP5K*γ-/- brains (17). Therefore, either PIP5Kγ is not a major

contributor to BMM's ambient PIP_2 pool in spite of its relative high abundance or its knockout induces compensatory changes in the activity of the other PIP5K isoforms or decreases overall PIP_2 turnover to maintain homeostasis.

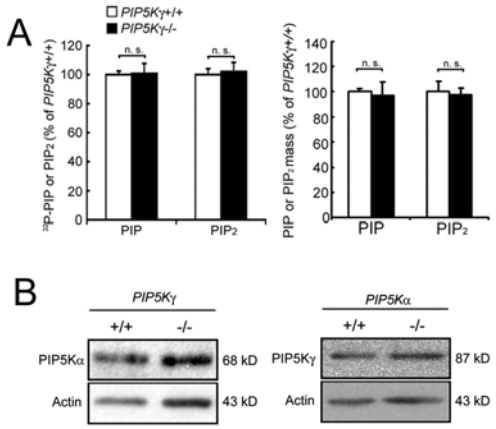

Figure 5. Phosphoinositide analyses and Western blot of BMM. (A) Phosphoinositide analyses. The PIP_2 or PIP value in *PIP5K*γ-/- BMM was expressed as % of WT cells. Left, TLC (n=3). Right, HPLC (n=4). (B) Western blot confirmed there was no compensatory increase of PIP5Kα in *PIP5K*γ-/- BMM and *vice versa*.

*PIP5K*γ-/- BMM HAVE ABNORMAL SHAPE AND ARE DEFECTIVE IN PHAGOCYTOSIS

BMM attached to coverslips were predominantly polygonal, while *PIP5K*γ-/- BMM were often elongated and stellate (Fig. 6A). *PIP5K*γ-/- BMM also had brighter phalloidin staining especially in the cell cortex. The bulk fluorometric phalloidin assay showed that there was a 50% increase in polymerized actin (Fig. 6B).

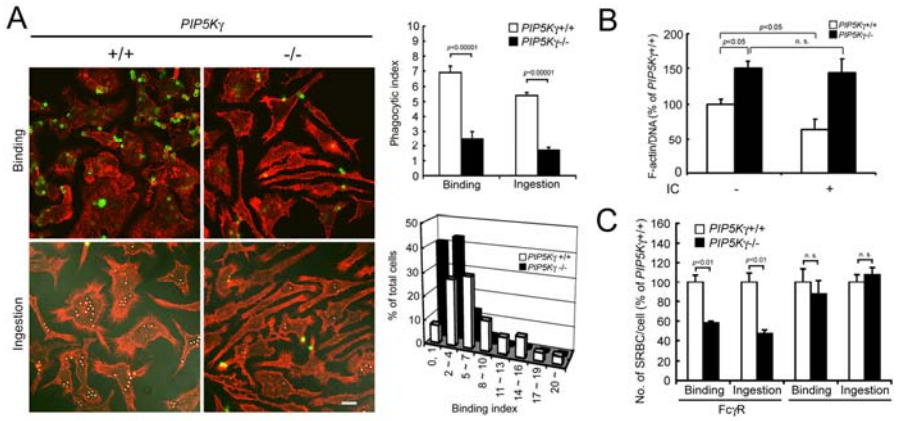

Figure 6. *PIP5K*γ-/- BMM are defective in attachment to IgG-opsonized particles. (A) Particle attachment and ingestion. Left, fluorescence/DIC images. DIC images were overlaid on the fluorescence images in the "ingestion" panels. External beads (green); phalloidin (red). Top right, phagocytic indices, defined as the average number of beads per cell (n>150 cells). Bottom right, particle attachment histogram. (B) IC-induced actin depolymerization. Polymerized actin was quantitated using a fluorometric phalloidin binding assay. The ratio of FITC-phalloidin to DAPI intensity was expressed as % of WT BMM without IC (n=6). (C) Selective inhibition of FcγR- but not C3R-mediated phagocytosis. BMM were incubated with either IgG- or C3bi-opsonized SRBC at 4ºC for 30 min without ("binding") or with a subsequent 37ºC incubation for 30 min ("ingestion"). The binding or ingestion index of WT BMM for each type of phagocytosis is set at 100%.

In addition, they phagocytized fewer IgG-opsonized particles (Fig. 6A). Using incubation at 4ºC vs. 37ºC to separate particle attachment (which can occur at 4ºC) from engulfment (which does not occur at 4ºC), I found that there was a marked decrease in particle binding (Fig. 6A). The binding index (mean number of attached particles/cell) decreased by 70% and the binding histogram shifted to the left (Fig. 6A). The decrease in particle attachment paralleled that of ingestion, suggesting that the primary defect resides in the initial attachment phase. Similar inhibition was observed using IgG-opsonized SRBC (Fig. 6C). Remarkably, *PIP5K*γ-/- BMM bound and ingested complement C3bi-opsonized SRBC normally (Fig. 2D). Thus, PIP5Kγ has a critical role

in the attachment phase of FcγR-mediated but not in C3 receptor (CR3)-mediated phagocytosis. The different requirement for PIP5Kγ is supported by previous observations that these two types of phagocytosis use different mechanisms of ingestion and regulation (200,204-206).

*PIP5K*γ-/- BMM HAVE IMPAIRED RESPONSES TO IC

The early zipper hypothesis proposes that particle attachment is mediated by the progressive interaction of FcγR with IgG (207). Recently, there is increasing evidence that receptor microclustering increases the avidity of the receptors for their ligands (192). FcγR, which contains an ITAM (9), oligomerizes to form microclusters (191). The role of actin in FcγR microclustering has not been examined. Here I investigated the possibility that the *PIP5K*γ-/- BMM's particle attachment defect is due to impaired FcγR microclustering by a static and excessively polymerized actin cytoskeleton.

Heat aggregated IC, which have been used extensively to ligate FcγR (9), was used to directly induce FcγR clustering and anti-IgG was used to detect the clusters (Fig. 7A). In WT BMM, IC binding was detected after 5 min incubation at 4ºC. By 20 min, the clusters became larger. Quantification by ImageJ showed that, on average, there was a 4.5-fold increase in cluster size (Fig. 7A). Similar results were obtained when FcγR were directly stained with 2.4G2 (Fig. 7B). In contrast, although IgG bound FcγR in *PIP5K*γ-/- BMM, the size of FcγR:IgG clusters did not increase substantially between 5

and 20 min (Fig. 7A). Therefore, receptor microclustering is impeded in *PIP5K*γ-/- BMM.

IC stimulation induced a 40% decrease in polymerized actin in WT BMM (Fig. 6B), providing evidence that FcγR ligation triggers dynamic actin rearrangements. In contrast, *PIP5K*γ-/- cells, which already had higher basal polymerized actin content, did not depolymerize their actin after IC stimulation (Fig. 6B). Taken together, my results suggest that *PIP5K*γ-/- BMM have a highly polymerized actin cytoskeleton that is static and impedes FcγR microclustering.

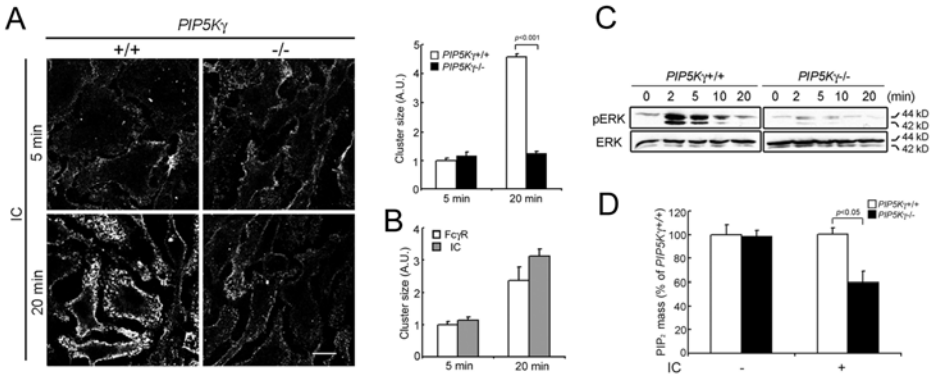

Figure 7. *PIP5K*γ-/- BMM are defective in response to IC. (A) IC-induced FcγR microclustering. BMM incubated with IC at 4ºC were stained with anti-IgG to detect FcγR clusters on the cell surface. Left, fluorescence images. Right, cluster size quantitation by ImageJ (n≈10000 clusters). Size was expressed in arbitrary units (A.U.) relative to WT BMM at 5 min. (B) Comparison of the use of anti-IgG vs. anti-FcγR to quantitate IC-induced microclustering. WT BMM were exposed to 100 μg/ml IC for 5 or 20 min at 4ºC. Cells were labeled with anti-human IgG or 2.4G2. The size of the clusters (n>1000) was analyzed with ImageJ software and calibrated as arbitrary unit (A.U.). (C) IC-induced ERK phosphorylation. BMM were exposed to IC at 4ºC for 20 min, washed, and incubated at 37ºC for the times indicated. ERK and pERK were detected by Western blot. (D) IC-induced change in PIP_2 homeostasis. BMM were challenged with or without IC for 2 min at 37ºC. The PIP_2 level was quantitated by HPLC and expressed as % of WT BMM without IC treatment (n=3).

FcγR ligation activates multiple downstream signaling pathways, including activation of the MAPK cascade, hydrolysis of PIP_2 by PLCγ and conversion of PIP_2 to PIP_3 by PI3Ks (9,192). IC stimulated ERK phosphorylation to a much lesser extent in *PIP5K*γ-/- BMM than in WT cells (Fig. 7C) and depleted the PIP_2 pool in knockout macrophages only (Fig. 7D). Attenuation of robust signal amplification is consistent with reduced FcγR microclustering but not a defect in the downstream ERK signaling cascade *per se*, because *PIP5K*γ-/- BMM phosphorylated ERK normally in response to CSF-1 (Fig. 4E). The differential effects of IC on WT and *PIP5K*γ-/- BMM PIP_2 level can be explained as follows. Although IC stimulates PIP_2 hydrolysis by PLCγ and conversion to PIP_3 by PI3Ks, the steady state PIP_2 level in WT BMM does not decrease because the pool is rapidly replenished. *PIP5K*γ-/- BMM could not refill the pool, as reflected in a 40% decrease in the amount of PIP_2 after IC stimulation. Additional experiments will be required to determine why loss of PIP5Kγ interfered with the normal ability of BMM to replenish the IC-depleted PIP_2 pool.

RESCUE OF *PIP5K*γ-/- BMM'S PHENOTYPES

I performed "rescue" experiments to establish a cause-and-effect relation between depletion of the PIP5Kγ-generated PIP_2 pool and the aberrant *PIP5K*γ-/- phenotypes. First, I attempted to rescue the abnormal cell shape and attenuated particle binding. Initially, I tried to do this by infecting BMM with retrovirus expressing GFP-PIP5Kγ87. However, less than 3% of the infected BMM expressed GFP-PIP5K, even

though 20% of cells expressed GFP alone. We then tried to "shuttle" PIP_2 into BMM instead (27,208). PIP_2 delivery corrected *PIP5K*γ-/- BMM's actin cytoskeletal and morphological defects (Fig. 8A) and restored their ability to bind particles (Fig 8B). Carrier alone had no effect. These results suggest that the shuttled PIP_2 can replenish the pool depleted by PIP5Kγ knockout and that the phenotypic changes are due to a decrease in PIP_2 generated by PIP5Kγ rather than a loss of PIP5Kγ protein or its scaffolding function *per se*.

Next I explored the relation between excessive actin polymerization and decreased particle attachment. Latr. B, which depolymerizes actin filaments, restored particle attachment to *PIP5K*γ-/- BMM at 0.05-0.2 μM, but had minimal effect on WT BMM (Fig. 8C). At 0.5 μM, Latr. B inhibited binding to WT BMM and was unable to rescue particle binding in *PIP5K*γ-/- BMM (Fig. 8C). Therefore, some actin polymerization is required for particle attachment, but too much inhibits. A biphasic requirement for polymerized actin has been reported previously in regulated exocytosis (209).

I also used Jasp. to block dynamic actin remodeling in WT BMM. Jasp. inhibited particle binding (Fig. 8D), IC clustering (Fig. 8E) and ERK activation (Fig. 8F). Since Jasp. treatment of WT BMM recapitulated multiple *PIP5K*γ-/- BMM's defects and low dose Latr. B rescued them in knockout cells, I conclude that controlled actin depolymerization facilitates FcγR microclustering, particle attachment and signal amplification and that PIP5Kγ generates the PIP_2 pool that regulates this depolymerization.

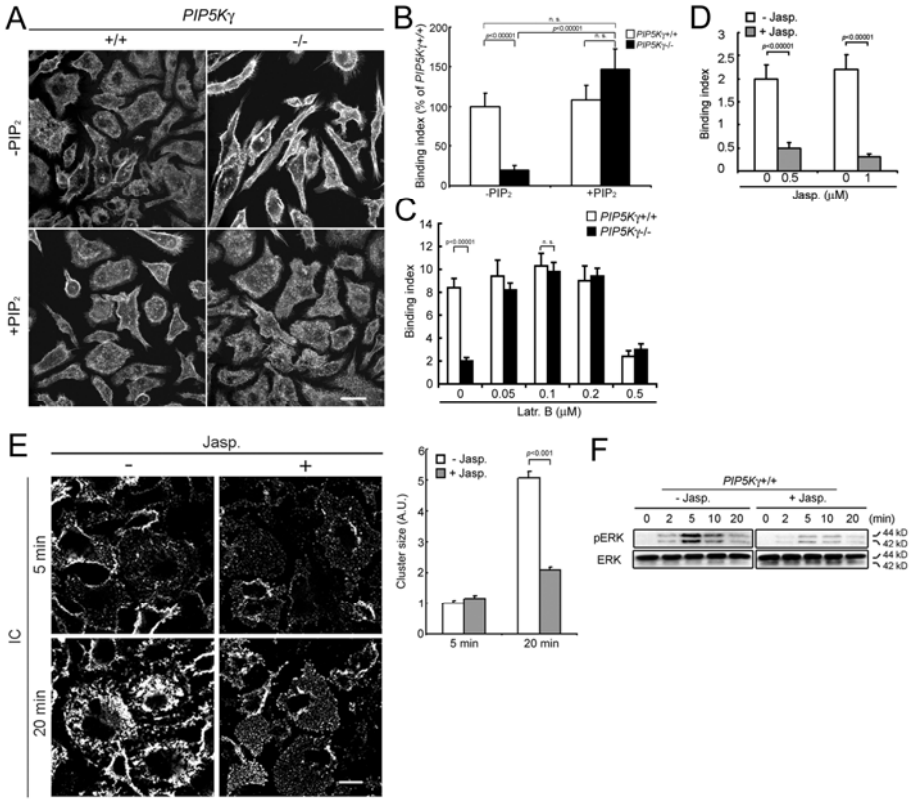

Figure 8. Relation between *PIP5Kγ* deficiency, actin, particle attachment and FcγR clustering defects. (A) Rescue of cell shape and actin by PIP_2 shuttling. BMM with or without exogenously added PIP_2 were stained with phalloidin. (B) Rescue of particle attachment by PIP_2 delivery. Binding indices (n>100) are expressed as % of WT BMM without PIP_2. (C) Rescue of particle attachment by Latr. B. Cells were incubated with Latr. B for 5 min at 37ºC before incubation with particles at 4ºC (n>70). (D) Inhibition of particle attachment to WT BMM by Jasp. Cells were incubated with 1 μM Jasp. at 37ºC for 30 min prior to the addition of IgG beads (n>50). (E) Inhibition of FcγR clustering in WT BMM by Jasp. Left, fluorescence staining of FcγR:IC clusters. Right, cluster size quantitation (n>1000). (F) Attenuation of IC-induced ERK phosphorylation by Jasp. Cells pretreated with or without Jasp. were incubated with IC at 4ºC for 20 min and warmed to 37ºC.

PIP5Kγ-/- BMM HAVE ABNORMAL RAC AND RHO ACTIVATION

Actin remodeling is regulated by a balance between the activation states of Rac and Rho GTPases (210). The *PIP5K*γ-/- actin phenotype could be explained by an alteration in GTPase activation or their downstream effector functions. To distinguish between these possibilities, I determined if PIP5Kγ knockdown disrupts Rac/Rho activation. GTPase effector pulldown assays showed that *PIP5K*γ-/- BMM had a 6-fold increase in GTP-RhoA and a 70% decrease in GTP-Rac1 (Fig. 9A). Thus, PIP5Kγ knockout altered RhoA and Rac1 activation in opposite directions to tip the balance towards RhoA domination.

To examine the relation between abnormal Rho/Rac activation, cytoskeletal and phagocytic defects, I manipulated the intracellular content of activated GTPases using multiple approaches. RhoA was inhibited by the cell permeable C3T. In WT BMM, C3T had no effect on binding at 5 μg/ml but inhibited at 10 μg/ml (Fig. 9B). Thus, some RhoA activity is required for normal particle attachment in WT cells. In contrast, C3T induced a dose-dependent increase in particle attachment to *PIP5K*γ-/- BMM and converted them from an extended stellate to a more "normal" polygonal shape (Fig. 9B). Therefore, excessive RhoA activation in *PIP5K*γ-/- BMM inhibits actin remodeling and contributes to their particle attachment and morphological defects.

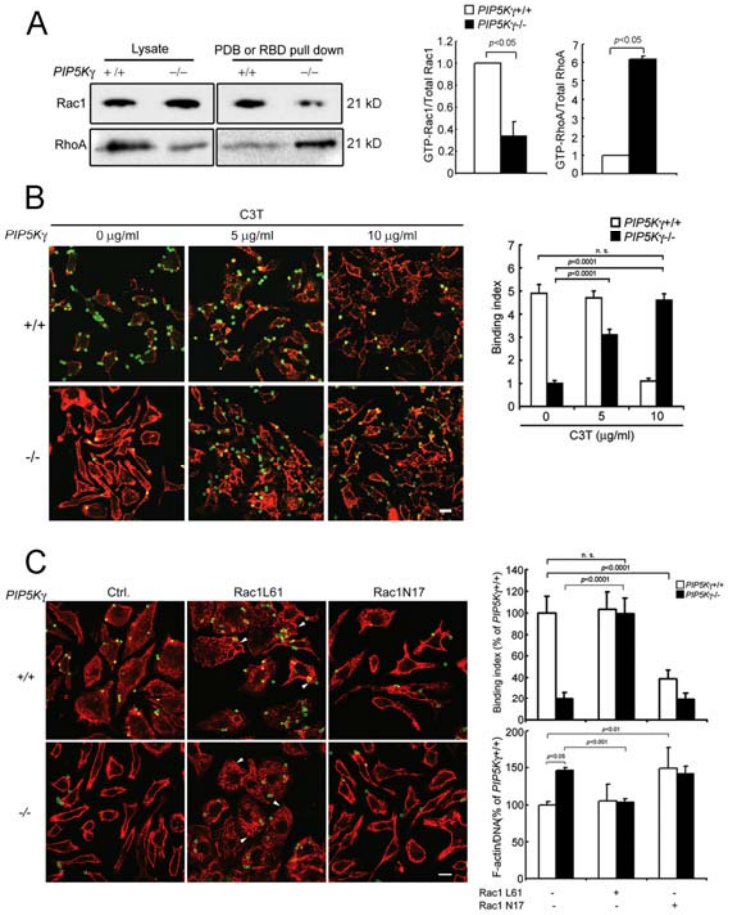

Figure 9. *PIP5K*γ-/- BMM have abnormal RhoA and Rac1 activation. (A) GTP-Rac1 or -RhoA pulldown by GST-PBD or -RBD, respectively. Samples were blotted with anti-Rac1 or -RhoA. Left, Western blot. Three times more WT BMM lysate and GST-RBD pulldown sample were loaded than *PIP5K*γ-/- BMM. Right, ratios of GTP-bound to total GTPase, expressed relative to that of WT BMM (n=4 for Rac1 and 2 for RhoA). (B) Rescue of particle biding defect by C3T. BMM were incubated with C3T at 37ºC for 4 h prior to the exposure of IgG-opsonized particles at 4ºC. Left, fluorescence staining. External beads (green); phalloidin (red). Right, binding indices (n>70). (C) Effects of manipulating Rac activation. BMM were transduced with 600 nM Tat-Rac1L61 or N17 at 37ºC for 30 min. Left, fluorescence images. External beads (green); phalloidin (red); arrowheads indicate dorsal ruffles. Right top, particle binding indices (n>50). Right bottom, fluorometric phalloidin quantitation (n=3). Data expressed as % of WT BMM without transduced Rac1.

Rac1 is the major Rac isoform in BMM (203,211) and it is activated during the early stages of cup formation and extension [reviewed in (10,212)]. Tat-based protein

transduction was used to introduce CA Rac1L61 and DN Rac1N17 (202). Rac1L61 converted the abnormally elongated *PIP5K*γ-/- BMM to a more normal polygonal shape, restored particle binding and decreased the amount of polymerized actin (Fig. 9C). It also induced the formation of dorsal ruffles in WT and *PIP5K*γ-/- BMM (Fig. 9C, arrowheads). Rac1N17 had no obvious effect on *PIP5K*γ-/- BMM, presumably because their endogenous Rac was already depressed in the absence of PIP5Kγ. However, Rac1N17 induced cell elongation, increased F-actin and decreased particle binding in WT BMM to recapitulate the *PIP5K*γ-/- phenotypes (Fig. 9C). The reciprocal effects on *PIP5K*γ-/- and WT BMM strongly suggest that Rac1 is necessary for particle attachment and that an imbalance of Rac1/RhoA contributes to *PIP5K*γ-/- BMM's particle attachment and morphological defects. The finding that inhibiting RhoA or increasing Rac1 activity is sufficient to rescue *PIP5K*γ-/- defects places PIP5Kγ upstream of RhoA/Rac1. This possibility has not been considered previously, since PIP5Ks are generally thought to be downstream effectors of Rho GTPases [reviewed in (14,41,148)].

*PIP5K*α-/- BMM ARE DEFECTIVE IN PARTICLE INGESTION

A *PIP5K*α-/- mouse line (human isoform designation; equivalent to mouse PIP5Kβ) has recently been generated (23). The *PIP5K*α-/- BMM did not express PIP5Kα (Fig. 10A) but had normal total and surface FcγR (Fig. 10A & B) and responded to CSF-1 by phosphorylating ERK normally (Fig. 10C). TLC analysis showed that there was a small (about 20%) but statistically significant decrease in ^{32}P-PIP_2. HPLC analysis

confirmed that the PIP_2 level was also decreased (Fig. 10D). Western blot showed that there was no compensatory change of PIP5Kγ (Fig. 5B), consistent with findings in *PIP5K*α-/- platelets (23).

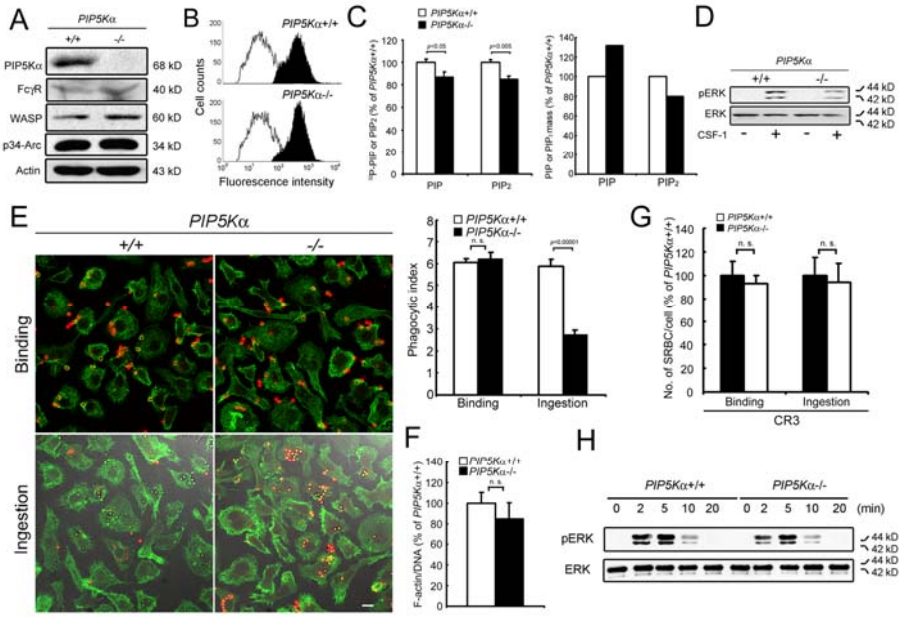

Figure 10. *PIP5K*α-/- BMM bind particles normally but ingest poorly. (A) Western blot. (B) FACs analysis of surface accessible FcγR. (C) Phosphoinositide profiles. Left, TLC (n=3). Right, HPLC from a representative experiment from two independent determinations. (D) CSF-1 induced ERK activation. (E) Particle attachment and ingestion. Left, fluorescence/DIC images. External beads (red); phallodin (green). Right, phagocytic indices (n≈70). (F) Fluorometric phalloidin quantitation (n=4). (G) CR3-mediated phagocytosis. (H) IC-induced ERK phosphorylation.

*PIP5K*α-/- BMM had no obvious change in cell shape or phalloidin actin staining (Fig. 10E). Fluorometric phalloidin quantitation confirmed that they had close to normal polymerized actin content (Fig. 10F). In addition, they bound IgG-opsonized particles (Fig. 10E), bound and ingested C3bi-opsonized SRBC (Fig. 10G), and phosphorylated ERK normally (Fig. 10H). Nevertheless, they had a 60% decrease in ingestion index

compared with WT BMM (Fig. 10E). Thus, PIP5Kα has a different role in phagocyosis than PIP5Kγ.

*PIP5K*α-/- BMM HAVE IMPAIRED ACTIN POLYMERIZATION DURING INGESTION

Particle ingestion is orchestrated by actin cytoskeletal changes during phagocytic cup initiation, cup extension, membrane closure and phagosome pinching off from the PM (10). Actin and PIP_2 are enriched in the nascent phagocytic cup and in the advancing pseudopodia during cup extension (59). I used immunofluorescence microscopy to determine if PIP5Kα knockout impaired actin accumulation at the phagocytic cups. Line scan of the fluorescent-phalloidin intensity from the base of the cup (x) to the contralateral PM (y) showed that there was a 2-fold and 1.2-fold enrichment (x/y ratio) in the cups in WT and *PIP5K*α-/- BMM (Fig. 11). Thus, although *PIP5K*α-/- BMM were able to initiate cup formation, their cups were shallower and were less efficient in mounting an actin polymerization response.

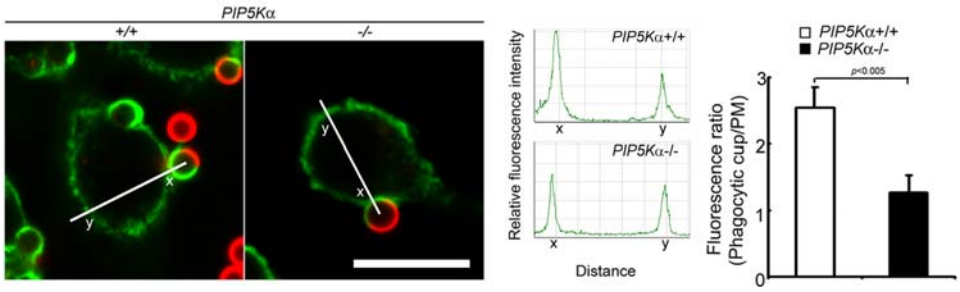

Figure 11. *PIP5K*α-/- BMM are defective in actin polymerization during ingestion. BMM incubated with IgG-opsonized beads at 4ºC for 10 min were warmed to 37ºC for 1 min. Quantitation of polymerized actin *in situ*. Left, fluorescence images. Phalloidin (green); external beads (red). Middle, line scans of phalloidin fluorescence intensity spanning the bottom of a nascent phagocytic cup (x) and its contralateral PM (y). Data shown were from representative cells. Right, ratio of phalloidin intensity (x/y) (n=30 cups).

I performed additional studies to determine if WASP-mediated activation of the Arp2/3 complex was compromised. WASP is required for efficient phagocytosis (197,213), and it is activated coordinately by PIP_2 and Cdc42 (214). Overexpression of PIP5K promotes WASP and Arp2/3 dependent actin polymerization (107). Using a WASP antibody that recognizes the active open conformation (198), I found that there was no detectible staining in the cytoplasm of WT BMM, but strong staining in the cups (Fig. 12A). On the other hand, the antibody that detects total WASP stained both the cups and cytoplasm (Fig. 12A, inset). Consistent with WASP activation in the cups, p34-Arc, a component of the Arp2/3 complex that binds active WASP, also accumulated there (Fig. 12B).

In contrast, only about 1% of the phagocytic cups in *PIP5K*α-/- BMM had active WASP (Fig. 12A) or p34-Arc staining (Fig. 12B), athough the knockout cells expressed normal amounts of WASP and Arp2/3 (Fig. 10A) and WASP *per se* was found in the cups (Fig. 12A, inset). I conclude that WASP is recruited to phagocytic cup

independently of PIP5Kα, but WASP activation is highly dependent on PIP5Kα. My results are in agreement with previous findings that WASP recruitment *per se* is not absolutely PIP_2-dependent [reviewed in (215)] and establish PIP5Kα as the primary source of PIP_2 for WASP activation in the cup.

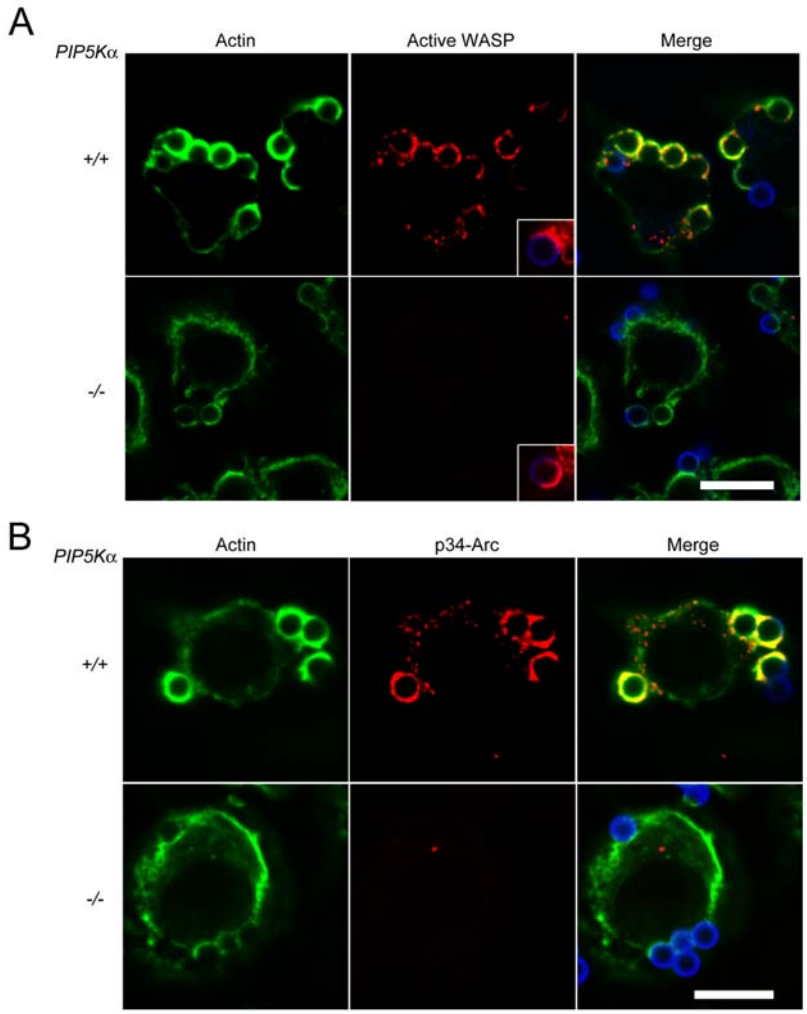

Figure 12. *PIP5K*α-/- BMM are defective in actin polymerization during ingestion. BMM incubated with IgG-opsonized beads at 4ºC for 10 min were warmed to 37ºC for 1 min. (A) Active WASP (red), phalloidin (green); external beads (blue). Inset, total WASP (red) in another cell. (B) p34-Arc (red).

PIP5Kα-/- BMM HAVE MEMBRANE RUFFLING DEFECTS

Having established that PIP5Kα initiates *de novo* actin polymerization at the phagocytic cup during ingestion, we investigated its role in the membrane ruffling process since PIP5Kα has been shown to be recruited to the membrane protrusions in mouse embryonic fibroblasts and locally generated PIP_2 is required for the cell migration (112). CSF-1 was used to induce membrane ruffle formation. We found that WT cells responded to CSF-1 stimulation by strongly ruffling their PM indicated by their wide and pedal-shaped peripheral membrane protrusions decorated by strong phalloidin staining. Whereas, much fewer *PIP5Kα*-/- cells exhibited the same response. Even in those that did, the size of the ruffles was notably smaller and the actin staining was dramatically decreased (Fig. 13A). Quantitation of ruffle index (mean number of ruffles/cell) confirmed that these cells had significantly fewer ruffles compared with WT cells (Fig. 13A). We also tested CSF-1 induced ERK activation and found that there was no apparent difference between *PIP5Kα*-/- and WT cells (Fig. 10D). Our results suggest that PIP5Kα is required for membrane ruffle formation but not the downstream ERK activation upon CSF-1 stimulation and that membrane ruffling and ERK activation are two independent pathways.

In contrast, response to CSF-1 in *PIP5Kγ*-/- BMM was normal (Fig. 13B). Without CSF-1 stimulation, *PIP5Kγ*-/- BMM were more elongated and had more F-actin compared with WT cells. However, cells still responded to CSF-1 by forming one or multiple peripheral membrane protrusions and some protrusions showed brighter phalloidin staining than those in WT cells. Ruffling index quantitation confirmed that

PIP5Kγ is not required during membrane ruffling (Fig. 13B). In addition, *PIP5K*γ-/- BMM also had normal ERK activation by CSF-1 (Fig. 4E) which was different from the IC stimulation (Fig. 7C). CSF-1 receptor is a tyrosine kinase receptor which dimerizes after ligand ligation (216), but whether CSF-1 signaling requires its further microclustering to sustain or propagate remains unknown. Our data suggest that FcγR and CSF-1 receptor have different sets of mechanisms to regulate its signal amplification and it merits further examination.

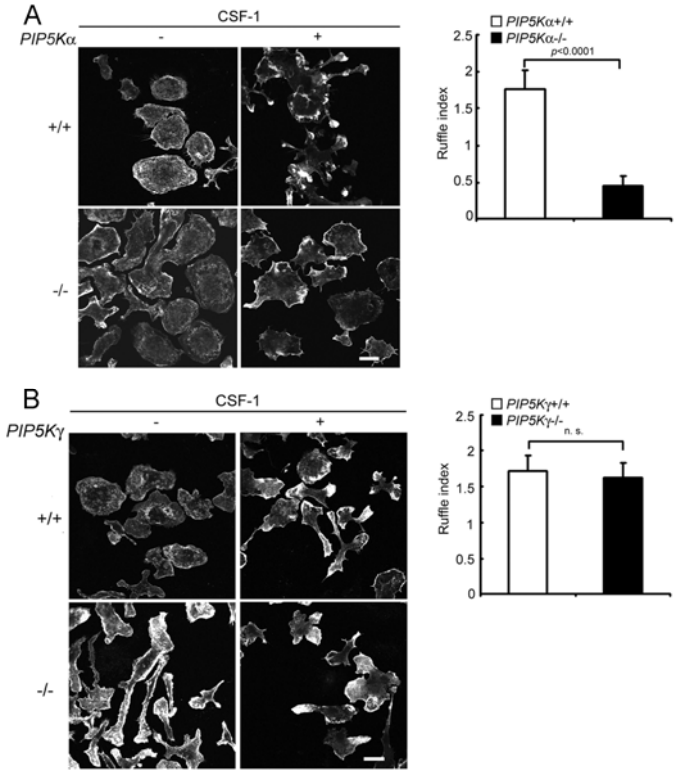

Figure 13. PIP5Kα and PIP5Kγ knockout have different effects on CSF-1-induced membrane ruffling. Left, immunofluorescent images of BMM stained with phalloidin. Right, ruffle index (n>30). (A) WT and *PIP5K*α-/- BMM. (B) WT and *PIP5K*γ-/- BMM.

PIP5Kγ AND α DEPLETION BY RNAI

My results from null mice provided definitive evidence for the differential roles of PIP5Kγ and α in actin remodeling after long term knockout. I next used RNAi to determine if depletion in the short term in another type of phagocytic cell has similar effects. Because BMM are difficult to transfect, I used the engineered phagocytic CHO-IIA cells, which stably express human FcγRIIA and phagocytize IgG-opsonized particles using a similar (albeit simpler) machinery (217). Compared with BMM, CHO-IIA cells had more PIP5Kα than PIP5Kγ (Fig. 2). PIP5K knockdown was confirmed by Western blot (Fig. 14A) and immunofluorescent staining (Fig. 14B). As in knockout BMM, surface FcγRIIA expression level did not change by PIP5Kα or γ knockdown (Fig. 14C) and PIP5Kα depletion decreased the PIP_2 level in CHO-IIA cells to a larger extent than PIP5Kγ depletion (Fig. 14D)

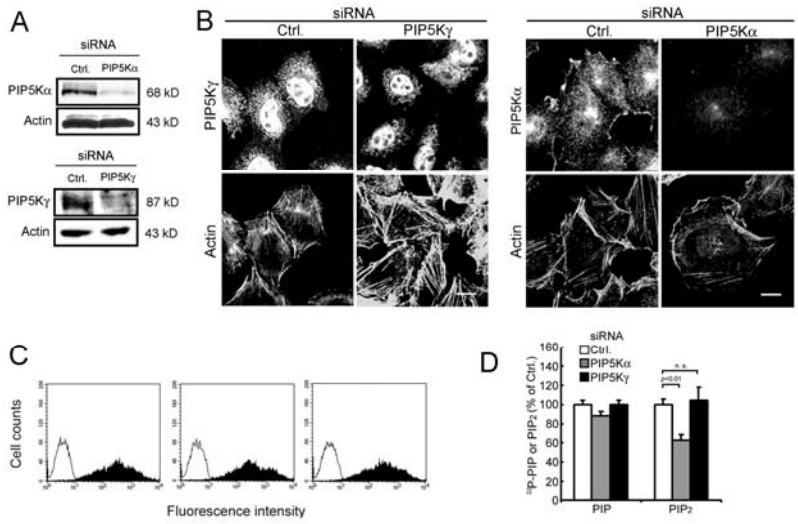

Figure 14. PIP5Kγ and α depletion by RNAi in CHO-IIA cells. (A) Western blot. The amount of lysate used for PIP5Kγ detection was 5 times higher than that for other proteins due to its low abundance. (B) Fluorescence images. Cells were stained with anti-PIP5Kγpan or α antibody and phalloidin. The anti-PIP5Kγpan staining in the nucleus was nonspecific and remained after RNAi. (C) FACs analysis of surface FcγRIIA in siRNA-transfected CHO-IIA cells. (D) TLC analysis (n=5).

The PIP5K depleted CHO-IIA cells exhibited phenotypic defects similar to those described above for the knockout BMM. PIP5Kγ knockdown decreased particle attachment, ingestion and FcγRIIA microclustering, while PIP5Kα knockdown decreased ingestion but had no effect on attachment (Fig. 15A) or microclustering (Fig. 15B). Like *PIP5Kα-/-* BMM, PIP5Kα depleted CHO-IIA cells form nascent phagocytic cups that had less polymerized actin (Fig. 16A) and less Arp2/3 enrichment (Fig. 16C), even though N-WASP (the WASP equivalent in non-hematopoietic cells) was present (Fig. 16D).

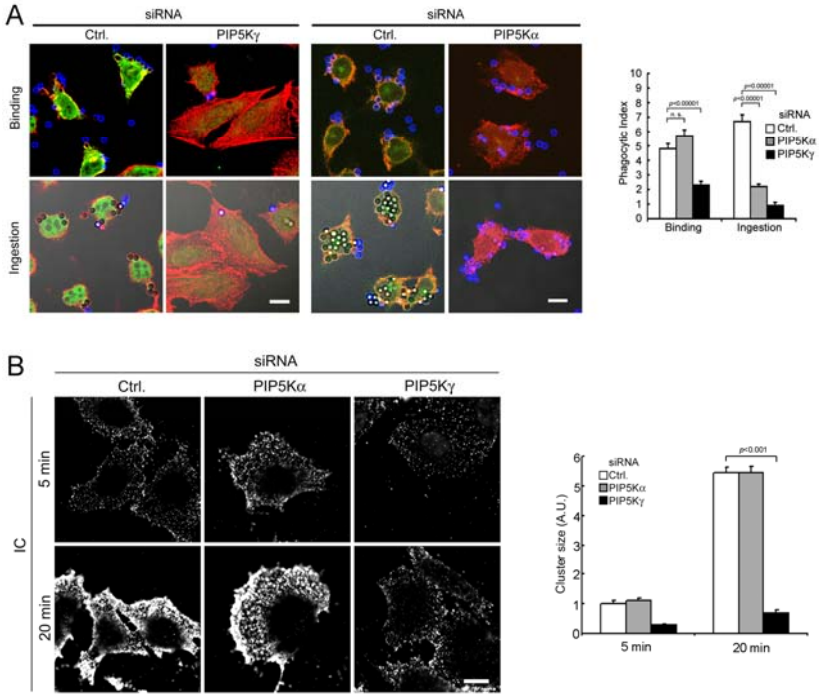

Figure 15. PIP5Kγ and α depletion's impact on phagocytosis and receptor clustering. (A) Particle attachment and ingestion. Left, fluorescence/DIC images. PIP5K (green); external beads (blue); phalloidin (red). Right, phagocytic indices (n>40). (B) IC-induced FcγRIIA microclustering in PIP5Kα and γ RNAi cells. Left, fluorescence images. Right, cluster size quantitation by ImageJ (n≈10000). Size was expressed in A.U. relative to Ctrl. RNAi cells at 5 min.

In control CHO-IIA cells, endogenous PIP5Kα and the transfected PIP_2 reporter, EGFP-PLCδ1 PH, were both enriched in the phagocytic cup (Fig. 16B, arrowheads), as shown previously (26). After PIP5Kα depletion, there was no detectible PIP5Kα in the cup. EGFP-PLCδ1PH was associated with the attached particles but its intensity was similar to that on the PM outside of the cups (Fig. 16B). Therefore, PIP5Kα is primarily responsible for the large focal increase in PIP_2 during cup formation. PIP5Kγ was not able to contribute to this PIP_2 pool.

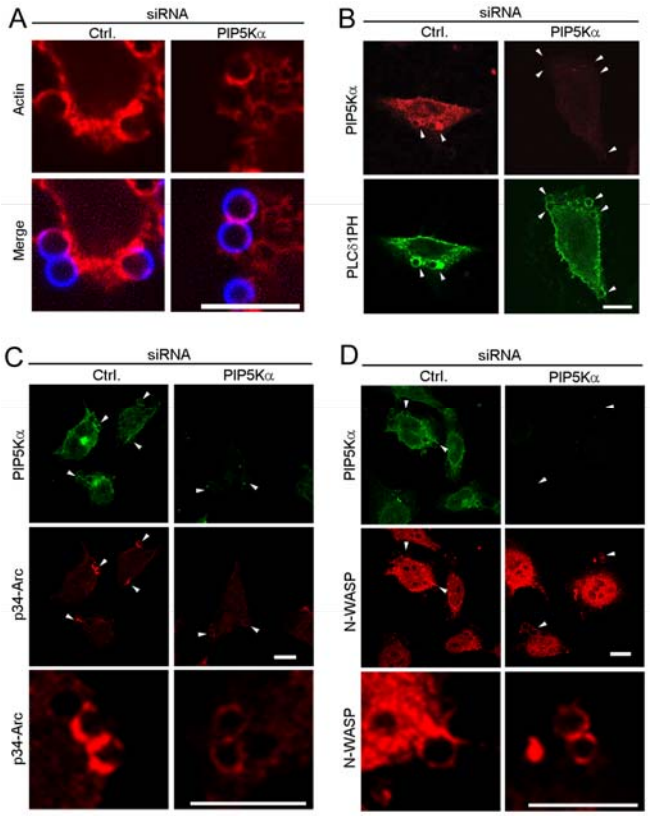

Figure 16. PIP5Kα depletion's impact on actin dynamics during ingestion in CHO-IIA cells.Recruitment of N-WASP and p34-Arc to phagocytic cup in PIP5Kα-depleted cells. Cells with prebound beads were incubated at 37ºC for 5 min. (A) Phalloidin staining. External beads (blue); phalloidin (red). (B) Endogenous PIP5Kα (red) and EGFP-PLCδ1PH (green). Arrowheads highlight phagocytic cups and particles being ingested. (C) PIP5Kα (green) and p34-Arc (red). (D) PIP5Kα (green) and N-WASP (red). Regions were shown at a higher magnification at the bottom panels.

PIP5Kγ BUT NOT α, IS TYROSINE PHOSPHORYLATED BY SYK DURING PHAGOCYTOSIS

The differential roles of PIP5Kγ and α can be most simply explained by their differential recruitment to phagocytic cup. However, immunofluorescence localization studies did not support this possibility. Within the limits of the resolution of my current approach, I found that both PIP5Ks were enriched in the nascent phagocytic cup and remained associated with the cup until completion of ingestion (Fig. 17). The conundrum of how these isoforms can exert independent and opposite control over the actin cytoskeleton in a sequential manner within the same restricted membrane region suggests that PIP5Ks may be subject to additional regulation.

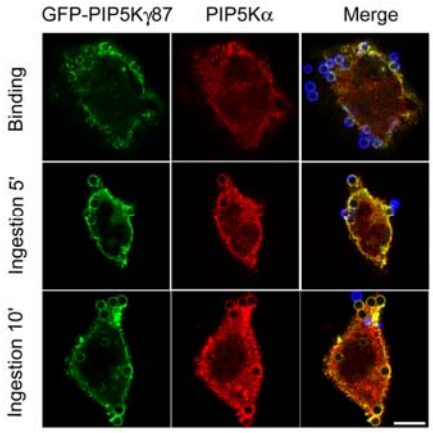

Figure 17. Colocalization of PIP5Kγ87 and α in CHO-IIA cells during phagocytosis. External beads (blue); endogenous PIP5Kα (red); overexpressed GFP-PIP5Kγ87 (green).

FcγR ligation activates Src family and Syk tyrosine kinases in tandem to initiate the phagocytic signaling cascade [reviewed in (9,192)]. PIP5Kγ87 and 90 were both tyrosine-phosphorylated when COS-IIA cells were stimulated with IgG, but not BSA, -opsonized particles (Fig. 18A). Phosphorylation peaked within 1-2 min and decreased thereafter. PIP5Kβ was also tyrosine phosphorylated but its phosphorylation peaked slightly later. In contrast, PIP5Kα was not detectibly tyrosine phosphorylated. Thus,

PIP5Ks are differentially regulated and transient PIP5Kγ tyrosine phosphorylation offers a potential explanation for the temporal regulation of its activity during phagocytosis. Because BMM, and the engineered phagocytic cells (CHO-IIA and COS-IIA) have much more PIP5Kγ87 than 90, I will focus on PIP5Kγ87 phosphorylation here.

Using a panel of tyrosine kinase inhibitors, I found that PIP5Kγ87 tyrosine phosphorylation was blocked by the Src inhibitor PP2 (Fig. 18B) and the Syk inhibitor piceatannol (Fig. 18B&C). Since Syk acts downstream of Src, I focused on the possibility that Syk is PIP5Kγ87's immediate physiological regulator. Syk is particularly abundant in hematopoietic cells, and is also found in many other types of cells, including COS cells (218). I used a DN Syk to block endogenous Syk in COS-IIA and found that it inhibited IgG induced increase in PIP5Kγ87 tyrosine phosphorylation (Fig. 18D). In addition, Syk phosphorylated PIP5Kγ87 *in vitro* and phosphorylation was blocked by piceatannol (Fig. 18E). Unexpectedly, although PIP5Kα was not tyrosine phosphorylated in cells, it was phosphorylated by Syk *in vitro* (Fig. 18E).

I used an *in vitro* lipid kinase assay to examine the effect of tyrosine phosphorylation on PIP5Kγ87's catalytic activity. PV, a potent tyrosine phosphatase inhibitor, was used to maximize tyrosine phosphorylation. Under conditions in which the rate of PIP_2 generation was linear, PIP5Kγ87 from PV-treated cells had a 2.3-fold higher specific activity than that from untreated cells (Fig. 18F). Taken together, these results established that PIP5Kγ is activated by Syk-mediated phosphorylation during phagocytosis.

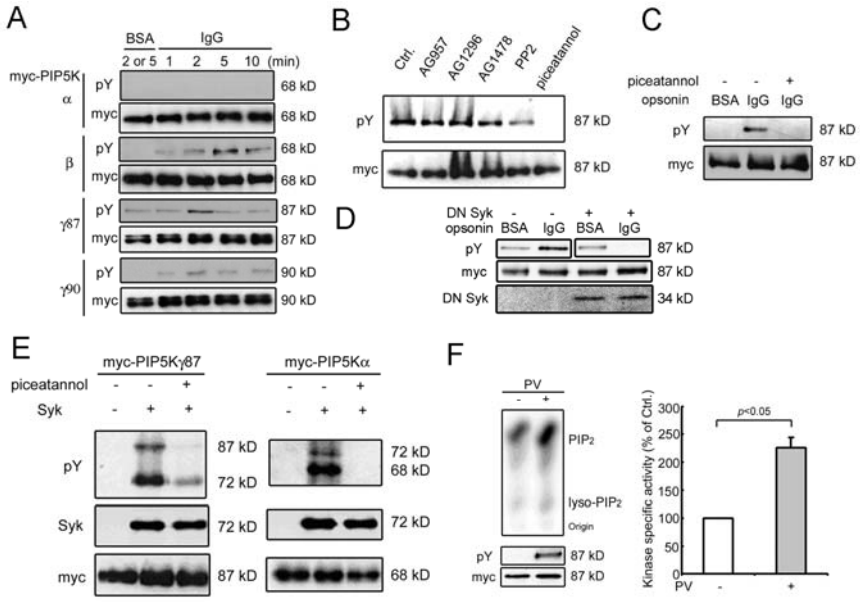

Figure 18. PIP5Kγ87 regulation by Syk. (A) Time course of PIP5K tyrosine phosphorylation. COS-IIA cells transfected with myc-PIP5K were challenged with BSA- or IgG-opsonized beads at 37ºC for different amounts of time. PIP5Ks were immunoprecipitated and Western blotted. (B) Effects of tyrosine kinase inhibitors on PIP5Kγ tyrosine phosphorylation. COS cells were transfected with PIP5Kγ87, incubated with various tyrosine kinase inhibitors for 1 h priot to the stimulation of 2 mM PV at 37ºC for 10 min, and lysed. PIP5Kγ87 was immunoprecipitated and Western blotted. (C) Effect of piceatannol. Myc-PIP5Kγ87 transfected COS-IIA cells were treated with or without 50 μM piceatannol for 30 min and challenged with BSA- or IgG-opsonized beads at 37ºC for 2 min. Immunoprecipitated myc-PIP5Kγ87 was immunoblotted. (D) Effect of DN Syk on myc-PIP5Kγ87 tyrosine phosphorylation. (E) *In vitro* tyrosine phosphorylation. Separately immunoprecipitated Syk and myc-PIP5Ks were incubated together with ATP. Phosphorylation was detected with anti-pY. (F) *In vitro* lipid kinase activity. Myc-PIP5Kγ87 immunoprecipitated from PV-treated COS cells were used for *in vitro* kinase assays. Left, autoradiogram of ^{32}P-labeled PIP_2 products after TLC (top) and Western blot of immunoprecipitated PIP5Kγ87 (bottom). Right, kinase specific activity (the amount of ^{32}P-PIP_2 generated in the linear portion of the kinase assay normalized against anti-myc intensity). The value from samples exposed to PV was expressed as % of that without PV (n=3).

PIP5Kγ BUT NOT α, IS ASSOCIATED WITH FCγR SIGNALOSOME

Since both PIP5Kγ and α can be tyrosine phosphorylated by Syk *in vitro*, but only PIP5Kγ exhibited tyrosine phosphorylation during phagocytosis *in vivo*. This paradoxical result raises the intriguing possibility that PIP5Kα, unlike PIP5Kγ, may not be accessible to Syk in the intact cell, even though both isoforms can be recruited to the phagocytic cups. In order to test this possibility, FcγR was transiently overexpressed with myc-PIP5Kγ or α in COS cells and immunoprecipitated after IC stimulation. Immunoprecipitates were blotted with anti-myc antibody and only PIP5Kγ, but not α, was found to be associated with FcγR signalosome complex (Fig. 19A).

Subsequently, two PIP5Kγ truncation mutants (aa 1-200 and aa 1-444) were tested to determine which region was responsible for its interaction. I found that both mutants were sufficient to interact with FcγR complex after IC stimulation (Fig. 19B). Therefore, I conclude that the N-terminal region of PIP5Kγ is sufficient to mediate its association with FcγR signalosome complex during phagocytosis. Further experiments were required to investigate the direct binding partner of PIP5Kγ in this complex, to map the minimum binding motif within PIP5Kγ, and to determine whether this motif is necessary for the interaction.

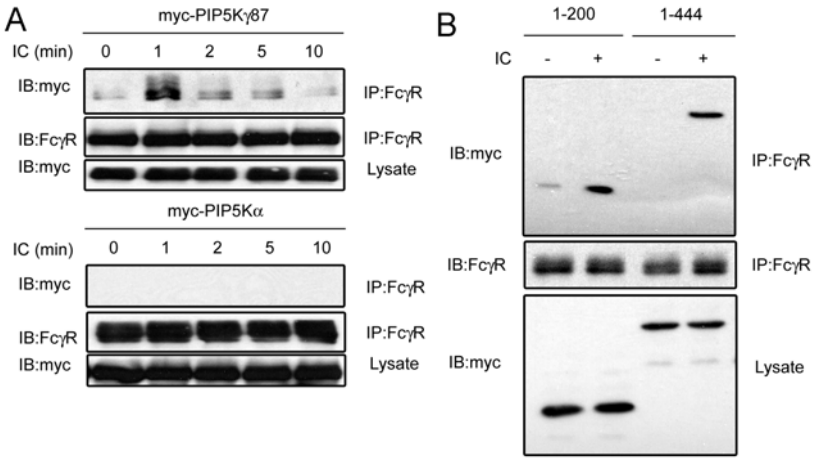

Figure 19. PIP5Kγ87 but not α associates with FcγR. (A) COS cells were transfected with FcγRIIA and myc-PIP5Kγ87 or α and stimulated for IC. FcγRIIA was immunoprecipitated and immunoprecipitates were Western blotted with anti-myc. (B) N-terminal region of PIP5Kγ is sufficient for its interaction with FcγR.

CHAPTER FIVE
Conclusions and Recommendations

PIP_2 regulates multiple biological processes at the PM [reviewed in (29,41)] and there is emerging evidence for the existence of functionally and/or spatially distinct PIP_2 pools contributed by different PIP5K isoforms [reviewed in (14)]. The prevailing hypothesis is that these PIP5Ks are differentially recruited to membrane sites by binding isoform-specific adaptors. For example, PIP5Kγ90 is recruited to focal adhesions by binding talin through its unique 28-amino acid COOH-terminal extension, while PIP5Kγ87, which lacks the COOH-terminal tail, is not (18,19). In addition, PIP5Kα is recruited to membrane ruffles by binding to Ajuba, a LIM protein (112).

Here I examined the role of PIP5Kγ and α in phagocytosis. I chose this model because it is orchestrated by temporally distinct steps that are dependent on dynamic changes in actin and PIP_2 within the confines of the phagocytic cup [reviewed in (10)]. PIP5Kγ and α are both recruited to the phagocytic cup and remain there until phagosome closure. I show that the temporal segregation of the processes they regulate, despite their apparent coexistence within the phagocytic cup, can be explained by their opposite effects on the actin cytoskeleton, their different placement within the small GTPase activation cascade and their differential regulation by Syk. My findings identify many novel aspects about the complex chain of events during phagocytosis and provide new insight into understanding other complex and dynamic PIP_2-dependent membrane processes.

PIP5K KNOCKOUT MICE

PIP5Kγ knockout, which is embryonically (20) or perinatally (17) lethal, induces severe neurological and cardiac development abnormalities. I cannot explain why these two lines of knockout mice die at different stages, but note that both have significant actin cytosekletal defects (17,24). Unlike the *PIP5K*γ-/- mice, the *PIP5K*α-/- mice have an implantation defect, but the occasional embryo that "escapes" survive to adulthood (23). I used PIP5Kγ-/- and α-/- BMM here and did not examine the role of PIP5Kβ, because BMM and CHO-IIA cells have very little PIP5Kβ and I were not able to obtain the PIP5Kβ knockout mice (25). Notably, *PIP5Kβ*-/- mice are viable, have no fertility defect and live a normal lifespan. The different effects of PIP5K knockout on mouse survival are consistent with their different *in vivo* roles.

PIP5Kγ AND α REGULATE DIFFERENT STEPS IN PHAGOCYTOSIS

PIP5Kγ knockout or RNAi increases the amount of polymerized actin under basal conditions and decreases the cytoskeleton's ability to depolymerize in response to FcγR ligation. These results support the actin "fence" model which proposes that the subplasmalemmal actin meshwork tethers transmembrane receptors to restrict their lateral diffusion (219). In this scenario, excessive actin polymerization, coupled with the inability to deploymerize in response to FcγR ligation, impede FcγR microclustering. Since other ITAM receptors, including TCR, BCR and mast cell FcεR also form

microclusters (193-196,220), I suggest that the initial actin depolymerization phase associated with their clustering may also be regulated by PIP5Kγ. Since PIP5Kγ87 is so much more abundant than γ90 in BMM and CHO-IIA cells, I assume that most of the phenotypic changes described here are due primarily to the loss of PIP5Kγ87. Additional experiments will be required to sort out the individual contributions of each PIP5Kγ isoform.

PIP5Kα knockout or RNAi had no effect on particle binding but inhibited particle ingestion. WASP was recruited to the phagocytic cups but was not activated. Therefore, PIP5Kα promotes WASP activation and WASP dependent *de novo* actin polymerization during particle ingestion. I speculate that actin polymerization during ingestion is facilitated by the abundant supply of actin monomers generated by PIP5Kγ during the initial attachment phase. However, since PIP5Kα and γ have opposite effects on actin polymerization, PIP5Kγ has to be tuned down in order for PIP5Kα to achieve net polymerization. I hypothesize that this is achieved through PIP5Kγ dephosphorylation.

PIP5KS ARE DIFFERENTIALLY REGULATED BY TYROSINE PHOSPHORYLATION

PIP5Ks have been implicated in many cellular functions, but there is surprisingly little information about how they are regulated by tyrosine phosphorylation. Up until now, only PIP5Kγ90 (3) and PIP5Kβ (40) are known to be tyrosine phosphorylated and there is no information about how any PIP5K isoform responds to FcγR ligation. Here I

show for the first time that PIP5Kγ87 is tyrosine phosphorylated and identified Syk, an apical master regulator of the phagocytic signaling cascade, as the immediate physiological regulator of PIP5Kγ87 during phagocytosis. PIP5Kγ regulation by Syk may provide cells with an elaborate positive feedforward signaling network at the particle binding stage. Significantly, since PIP5Kγ87 is transiently phosphorylated, this will generate a spike of PIP_2 to drive actin depolymerization during receptor ligation and PIP5Kγ87 subsequently dialed down to allow PIP5Kα-initiated actin polymerization to dominate during particle engulfment.

I do not know at present if PIP5Kα activity is modulated during phagocytosis. Unlike PIP5Kγ, PIP5Kα is not tyrosine-phosphorylated in cells even though it can be phosphorylated by Syk *in vitro.* Since PIP5Kα and γ coexist in the nascent phagocytic cup, this would imply that Syk may have differential access to these PIP5Ks. Because FcγR microclusters are recruited into Src-containing raft microdomains and the Src-phosphorylated FcγR recruits Syk (221,222), I speculate that PIP5Kγ, but not PIP5Kα, is also preferentially recruited to raft microdomains. Consistently, my results established that the N-terminal region of PIP5Kγ mediates its association with FcγR signalosome complex followed by receptor activation. This region is absent in other PIP5K isoforms which explains why PIP5Kα is unable to interact with the signalosome complex and therefore cannot be tyrosine phosphorylated. The regulation of PIP5Kγ87 activity by tyrosine phosphorylation may also explain why even though BMM have abundant PIP5Kγ87, PIP5Kγ knockout does not decrease the amount of PIP_2 significantly. Perhaps

PIP5Kγ87 is not maximally active under ambient conditions. Full activation may require its recruitment to the PM as well as tyrosine phosphorylation.

RELATIONS BETWEEN RAC1, RHOA AND PIP5KS

Rac promotes *de novo* actin polymerization during internalization (10). Rho, which increases stress fibers in fibroblasts, has been implicated in the regulation of FcγR-mediated phagocytosis by some (200,223) but not other studies (204,206). Recently, Hall *et. al.* found that high dose C3T significantly inhibits FcγR-mediated phagocytosis, by an as yet identified mechanism that is not mediated through the actin cytoskeleton (200). I find that extensive Rho inhibition or actin depolymerization inhibits particle attachment, establishing definitively that Rho does regulate FcγR-mediated phagocytosis; low level Rho activity is required to maintain a minimal level of actin polymerization to induce FcγR microclustering, while too much Rho inhibits.

My results show that Rac1 and RhoA have reciprocal roles in the particle attachment step, as they do in other processes (210). *PIP5K*γ-/- BMM have less GTP-Rac1 and more GTP-RhoA and their phagocytic defects are rescued by inhibiting RhoA with C3T or by transducing the CA Rac1L61. Since rescue occurs in the absence of PIP5Kγ, I conclude that PIP5Kγ acts upstream of Rac and Rho. This placement is different from previous models based on the assumption that PIP5Ks act exclusively downstream of these GTPases [reviewed in (14,41,148)]. The prevailing model is based on the following findings: first, PIP5Ks bind Rho GTPases in GST-pull down assays,

although binding is not dependent on GTPase activation (151); second, Rho GTPases increase PIP5K membrane recruitment and, in some cases, activity (109,150,224). My placement of PIP5Kγ upstream of Rho/Rac activation does not preclude its additional regulation by GTPases further downstream (Fig. 19). Also, based on previously published results, and PIP5Kα's role in WASP activation, I place PIP5Kα downstream of Rac/Cdc42 activation.

Additional experiments will be required to determine how PIP5Kγ regulates Rac/Rho activation. I speculate that it may activate Rac1 and suppress RhoA by altering the balance between their respective guanine nucleotide exchange factors, GTPase activating proteins and guanine nucleotide dissociation inhibitors. These may include inactivation of p190RhoGAP and activation of the RacGEF DOCK180 that have been implicated in phagocytosis (225,226). There is a recent example of an interplay between PIP5Kβ and a RhoGDI to activate RhoA (146).

THE MODEL FOR THE DIFFERENTIAL ROLES OF PIP5KS DURING PHAGOCYTOSIS

To summarize, I have established a role of PIP5Kγ in maintaining the balance between Rac/Rho activation and in dynamic remodeling of the actin cytoskeleton to promote FcγR clustering, particle attachment and signal propagation. I show that the *PIP5K*γ-/- phenotype is due to the loss of the PIP5Kγ-generated PIP_2 pool. I have also established a role of PIP5Kα in activating WASP to induce *de novo* actin polymerization

in the phagocytic cup. I propose the following working model (Fig. 20). Under basal conditions, PIP5Kγ maintains a dynamic actin cytoskeleton. FcγR binding to IgG recruits PIP5Kγ to the site of particle attachment. PIP5Kγ initiates controlled actin depolymerization, by tilting the Rho family GTPase balance towards increased Rac activation. Dynamic actin remodeling releases the "tethering" of FcγR by the subplasmalemmal actin cytoskeleton to facilitate receptor oligomerization. Receptor microclustering robustly activates Syk, which further activates PIP5Kγ by tyrosine phosphorylation in a positive feedforward manner. The overall effect is an increase in the avidity of FcγR for IgG to promote stable particle attachment and signal amplification. This stages the attachment site for the subsequent ingestion step by generating an abundant supply of actin monomers to fuel *de novo* actin polymerization. PIP5Kγ is tuned down by dephosphorylation and PIP5Kα generates PIP_2 at the nascent phagocytic cup to recruit Arp2/3 by activating WASP. Unlike PIP5Kγ, PIP5Kα is likely to act primarily downstream of Rac/Cdc42 and it is not phosphorylated by Syk.

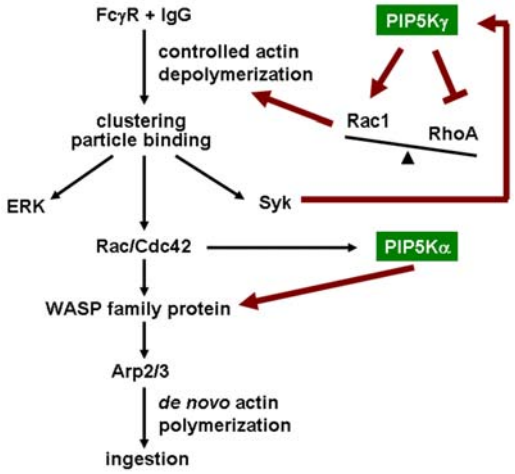

Figure 20. Model for the unique roles and differential regulations of PIP5Kγ and α in FcγR-mediated phagocytosis. Controlled actin depolymerization is initiated upon FcγR ligation to IgG. PIP5Kγ activates Rac and inhibits Rho, tilting the balance towards actin disassembly. Actin remodeling releases the "tethering" of FcγR to promote formation of FcγR microclusters which promote particle binding and downstream signaling including ERK and Syk activation. Syk further phosphorylates and activates PIP5Kγ in a positive feedforward manner. PIP5Kα generates PIP_2 at the nascent phagocytic cup to activate WASP family proteins. Arp2/3 binds activated WASP and initiates *de novo* actin polymerization for particle ingestion. Our model places PIP5Kγ upstream of Rac/Rho based on data presented here and PIP5Kα downstream of Rac/Cdc42 based on previous published results and PIP5Kα's role in WASP activation described here. Our model does not preclude additional feedback regulation of PIP5Kγ by these small GTPases.

BIBLIOGRAPHY

1. Park, S. J., Itoh, T., and Takenawa, T. (2001) *J. Biol. Chem.* **276**, 4781-4787
2. Itoh, T., Ishihara, H., Shibasaki, Y., Oka, Y., and Takenawa, T. (2000) *J. Biol. Chem.* **275**, 19389-19394
3. Ling, K., Doughman, R. L., Iyer, V. V., Firestone, A. J., Bairstow, S. F., Mosher, D. F., Schaller, M. D., and Anderson, R. A. (2003) *J. Cell Biol.* **163**, 1339-1349
4. Sun, Y., Ling, K., Wagoner, M. P., and Anderson, R. A. (2007) *J Cell Biol* **178**, 297-308
5. Bairstow, S. F., Ling, K., and Anderson, R. A. (2005) *J. Biol. Chem.* **280**, 23884-23891
6. Nakano-Kobayashi, A., Yamazaki, M., Unoki, T., Hongu, T., Murata, C., Taguchi, R., Katada, T., Frohman, M. A., Yokozeki, T., and Kanaho, Y. (2007) *Embo J* **26**, 1105-1116
7. Lee, S. Y., Voronov, S., Letinic, K., Nairn, A. C., Di Paolo, G., and De Camilli, P. (2005) *J. Cell Biol.* **168**, 789-799
8. Groves, E., Dart, A. E., Covarelli, V., and Caron, E. (2008) *Cellular and molecular life sciences* **65**, 1957-1976
9. Nimmerjahn, F., and Ravetch, J. V. (2008) *Nat Rev Immunol* **8**, 34-47
10. Swanson, J. A. (2008) *Nat Rev Mol Cell Biol* **9**, 639-649
11. Botelho, R. J., Teruel, M., Dierckman, R., Anderson, R., Wells, A., York, J. D., Meyer, T., and Grinstein, S. (2000) *J. Cell Biol.* **151**, 1353-1368
12. Yeung, T., Terebiznik, M., Yu, L., Silvius, J., Abidi, W. M., Philips, M., Levine, T., Kapus, A., and Grinstein, S. (2006) *Science* **313**, 347-351
13. Corbett-Nelson, E. F., Mason, D., Marshall, J. G., Collette, Y., and Grinstein, S. (2006) *J Cell Biol* **174**, 255-265
14. Mao, Y. S., and Yin, H. L. (2007) *Pflugers Arch* **455**, 5-18
15. Ishihara, H., Shibasaki, Y., Kizuki, N., Wada, T., Yazaki, Y., Asano, T., and Oka, Y. (1998) *J. Biol. Chem.* **273**, 8741-8748
16. Wang, Y. J., Li, W. H., Wang, J., Xu, K., Dong, P., Luo, X., and Yin, H. L. (2004) *J. Cell Biol.* **167**, 1005-1010
17. Di Paolo, G., Moskowitz, H. S., Gipson, K., Wenk, M. R., Voronov, S., Obayashi, M., Flavell, R., Fitzsimonds, R. M., Ryan, T. A., and De Camilli, P. (2004) *Nature* **431**, 415-422
18. Di Paolo, G., Pellegrini, L., Letinic, K., Cestra, G., Zoncu, R., Voronov, S., Chang, S., Guo, J., Wenk, M. R., and De Camilli, P. (2002) *Nature* **420**, 85-89
19. Ling, K., Doughman, R. L., Firestone, A. J., Bunce, M. W., and Anderson, R. A. (2002) *Nature* **420**, 89-93
20. Wang, Y., Lian, L., Golden, J. A., Morrisey, E. E., and Abrams, C. S. (2007) *Proceedings of the National Academy of Sciences of the United States of America* **104**, 11748-11753
21. Padron, D., Wang, Y. J., Yamamoto, M., Yin, H., and Roth, M. G. (2003) *J. Cell Biol.* **162**, 693-701

22. Micucci, F., Capuano, C., Marchetti, E., Piccoli, M., Frati, L., Santoni, A., and Galandrini, R. (2008) *Blood* **111**, 4165-4172
23. Wang, Y., Chen, X., Lian, L., Tang, T., Stalker, T. J., Sasaki, T., Brass, L. F., Choi, J. K., Hartwig, J. H., and Abrams, C. S. (2008) *Proceedings of the National Academy of Sciences of the United States of America* **105**, 14064-14069
24. Wang, Y., Litvinov, R. I., Chen, X., Bach, T. L., Lian, L., Petrich, B. G., Monkley, S. J., Critchley, D. R., Sasaki, T., Birnbaum, M. J., Weisel, J. W., Hartwig, J., and Abrams, C. S. (2008) *J Clin Invest* **118**, 812-819
25. Sasaki, J., Sasaki, T., Yamazaki, M., Matsuoka, K., Taya, C., Shitara, H., Takasuga, S., Nishio, M., Mizuno, K., Wada, T., Miyazaki, H., Watanabe, H., Iizuka, R., Kubo, S., Murata, S., Chiba, T., Maehama, T., Hamada, K., Kishimoto, H., Frohman, M. A., Tanaka, K., Penninger, J. M., Yonekawa, H., Suzuki, A., and Kanaho, Y. (2005) *J. Exp. Med.* **201**, 859-870
26. Coppolino, M. G., Dierckman, R., Loijens, J., Collins, R. F., Pouladi, M., Jongstra-Bilen, J., Schreiber, A. D., Trimble, W. S., Anderson, R., and Grinstein, S. (2002) *J. Biol. Chem.* **277**, 43849-43857
27. Wang, Y. J., Wang, J., Sun, H. Q., Martinez, M., Sun, Y. X., Macia, E., Kirchhausen, T., Albanesi, J. P., Roth, M. G., and Yin, H. L. (2003) *Cell* **114**, 299-310
28. Roth, M. G. (2004) *Physiol. Rev.* **84**, 699-730
29. Di Paolo, G., and De Camilli, P. (2006) *Nature* **443**, 651-657
30. Heo, W. D., Inoue, T., Park, W. S., Kim, M. L., Park, B. O., Wandless, T. J., and Meyer, T. (2006) *Science* **314**, 1458-1461
31. Sheetz, M. P., Sable, J. E., and Dobereiner, H. G. (2006) *Annu Rev Biophys Biomol Struct* **35**, 417-434
32. Hilgemann, D. W., Feng, S., and Nasuhoglu, C. (2001) *Sci. STKE* **2001**, re19-
33. Suh, B.-C., and Hille, B. (2005) *Current Opinion in Neurobiology* **15**, 370-378
34. Krauss, M., and Haucke, V. (2007) *EMBO Rep* **8**, 241-246
35. Martin, T. F. J. (2001) *Current Opinion in Cell Biology* **13**, 493-499
36. DeMali, K. A., Wennerberg, K., and Burridge, K. (2003) *Current Opinion in Cell Biology* **15**, 572-582
37. Logan, M. R., and Mandato, C. A. (2006) *Biol. Cell* **98**, 377-388
38. Martin-Belmonte, F., Gassama, A., Datta, A., Yu, W., Rescher, U., Gerke, V., and Mostov, K. (2007) *Cell* **128**, 383-397
39. Mejillano, M., Yamamoto, M., Rozelle, A. L., Sun, H.-Q., Wang, X., and Yin, H. L. (2001) *J. Biol. Chem.* **276**, 1865-1872
40. Halstead, J. R., van Rheenen, J., Snel, M. H. J., Meeuws, S., Mohammed, S., D'Santos, C. S., Heck, A. J., Jalink, K., and Divecha, N. (2006) *Current Biology* **16**, 1850-1856
41. Yin, H. L., and Janmey, P. A. (2003) *Annual Review of Physiology* **65**, 761-789
42. Hilpela, P., Vartiainen, M. K., and Lappalainen, P. (2004) *Curr Top Microbiol Immunol* **282**, 117-163
43. Sechi, A. S., and Wehland, J. (2000) *J Cell Sci* **113**, 3685-3695
44. Divecha, N., and Irvine, R. F. (1995) *Cell* **80**, 269-278
45. McLaughlin, S., and Murray, D. (2005) *Nature* **438**, 605-611

46. Homma, K., Terui, S., Minemura, M., Qadota, H., Anraku, Y., Kanaho, Y., and Ohya, Y. (1998) *J. Biol. Chem.* **273**, 15779-15786
47. Rao, V. D., Misra, S., Boronenkov, I. V., Anderson, R. A., and Hurley, J. H. (1998) *Cell* **94**, 829-839
48. Kunz, J., Fuelling, A., Kolbe, L., and Anderson, R. A. (2002) *J. Biol. Chem.* **277**, 5611-5619
49. Toker, A., and Cantley, L. C. (1997) *Nature* **387**, 673-676
50. Stephens, L. R., Hughes, K. T., and Irvine, R. F. (1991) *Nature* **351**, 33-39
51. Rhee, S. G. (2001) *Annu Rev Biochem* **70**, 281-312
52. Franca-Koh, J., Kamimura, Y., and Devreotes, P. N. (2007) *Nat Cell Biol* **9**, 15-17
53. Wymann, M. P., and Marone, R. (2005) *Current Opinion in Cell Biology* **17**, 141-149
54. Astle, M. V., Horan, K. A., Ooms, L. M., and Mitchell, C. A. (2007) *Biochem Soc Symp*, 161-181
55. Perera, R. M., Zoncu, R., Lucast, L., De Camilli, P., and Toomre, D. (2006) *PNAS* **103**, 19332-19337
56. Dressman, M. A., Olivos-Glander, I. M., Nussbaum, R. L., and Suchy, S. F. (2000) *J. Histochem. Cytochem.* **48**, 179-190
57. Brown, F. D., Rozelle, A. L., Yin, H. L., Balla, T., and Donaldson, J. G. (2001) *J. Cell Biol.* **154**, 1007-1018
58. Cremona, O., and De Camilli, P. (2001) *J Cell Sci* **114**, 1041-1052
59. Scott, C. C., Dobson, W., Botelho, R. J., Coady-Osberg, N., Chavrier, P., Knecht, D. A., Heath, C., Stahl, P., and Grinstein, S. (2005) *J. Cell Biol.* **169**, 139-149
60. Balla, T., and Varnai, P. (2002) *Sci STKE* **2002**, PL3
61. Laux, T., Fukami, K., Thelen, M., Golub, T., Frey, D., and Caroni, P. (2000) *J. Cell Biol.* **149**, 1455-1472
62. Raucher, D., Stauffer, T., Chen, W., Shen, K., Guo, S., York, J. D., Sheetz, M. P., and Meyer, T. (2000) *Cell* **100**, 221-228
63. Funaki, M., DiFransico, L., and Janmey, P. A. (2006) *Biochimica et Biophysica Acta (BBA) - Molecular Cell Research* **1763**, 889-899
64. Suh, B.-C., Inoue, T., Meyer, T., and Hille, B. (2006) *Science* **314**, 1454-1457
65. Varnai, P., Thyagarajan, B., Rohacs, T., and Balla, T. (2006) *J. Cell Biol.* **175**, 377-382
66. van Zeijl, L., Ponsioen, B., Giepmans, B. N., Ariaens, A., Postma, F. R., Varnai, P., Balla, T., Divecha, N., Jalink, K., and Moolenaar, W. H. (2007) *J Cell Biol* **177**, 881-891
67. Hao, J. J., Liu, Y., Kruhlak, M., Debell, K. E., Rellahan, B. L., and Shaw, S. (2009) *J Cell Biol* **184**, 451-462
68. Pan, W., Choi, S. C., Wang, H., Qin, Y., Volpicelli-Daley, L., Swan, L., Lucast, L., Khoo, C., Zhang, X., Li, L., Abrams, C. S., Sokol, S. Y., and Wu, D. (2008) *Science* **321**, 1350-1353
69. Hirose, K., Kadowaki, S., Tanabe, M., Takeshima, H., and Iino, M. (1999) *Science* **284**, 1527-1530

70. Brown, D. A., Hughes, S. A., Marsh, S. J., and Tinker, A. (2007) *J Physiol* **582**, 917-925
71. Hughes, S., Marsh, S. J., Tinker, A., and Brown, D. A. (2007) *Pflugers Arch* **455**, 115-124
72. Golub, T., and Caroni, P. (2005) *J. Cell Biol.* **169**, 151-165
73. Pike, L. J., and Miller, J. M. (1998) *J. Biol. Chem.* **273**, 22298-22304
74. Morris, J. B., Huynh, H., Vasilevski, O., and Woodcock, E. A. (2006) *Journal of Molecular and Cellular Cardiology* **41**, 17-25
75. Osawa, S., Funamoto, S., Nobuhara, M., Wada-Kakuda, S., Shimojo, M., Yagishita, S., and Ihara, Y. (2008) *J Biol Chem* **283**, 19283-19292
76. Yeo, D. S., Chan, R., Brown, G., Ying, L., Sutejo, R., Aitken, J., Tan, B. H., Wenk, M. R., and Sugrue, R. J. (2009) *Virology*
77. Aoyagi, K., Sugaya, T., Umeda, M., Yamamoto, S., Terakawa, S., and Takahashi, M. (2005) *J. Biol. Chem.* **280**, 17346-17352
78. Milosevic, I., Sorensen, J. B., Lang, T., Krauss, M., Nagy, G., Haucke, V., Jahn, R., and Neher, E. (2005) *J. Neurosci.* **25**, 2557-2565
79. Tong, J., Nguyen, L., Vidal, A., Simon, S. A., Skene, J. H., and McIntosh, T. J. (2008) *Biophys J* **94**, 125-133
80. Yang, S. A., Carpenter, C. L., and Abrams, C. S. (2004) *J Biol Chem* **279**, 42331-42336
81. Saito, K., Tolias, K. F., Saci, A., Koon, H. B., Humphries, L. A., Scharenberg, A., Rawlings, D. J., Kinet, J.-P., and Carpenter, C. L. (2003) *Immunity* **19**, 669-677
82. Kobayashi, T., Takematsu, H., Yamaji, T., Hiramoto, S., and Kozutsumi, Y. (2005) *J. Biol. Chem.* **280**, 18087-18094
83. Shaw, A. S. (2006) *Nat Immunol* **7**, 1139-1142
84. Cho, H., Kim, Y. A., Yoon, J.-Y., Lee, D., Kim, J. H., Lee, S. H., and Ho, W.-K. (2005) *PNAS* **102**, 15241-15246
85. Johnson, C. M., Chichili, G. R., and Rodgers, W. (2008) *J Biol Chem* **283**, 29920-29928
86. Stossel, T. P., Fenteany, G., and Hartwig, J. H. (2006) *J Cell Sci* **119**, 3261-3264
87. Condeelis, J. (2001) *Trends in Cell Biology* **11**, 288-293
88. Higgs, H. N., and Pollard, T. D. (2001) *Annual Review of Biochemistry* **70**, 649-676
89. Lemmon, M. A. (2003) *Traffic* **4**, 201-213
90. Pearson, M. A., Reczek, D., Bretscher, A., and Karplus, P. A. (2000) *Cell* **101**, 259-270
91. Janmey, P. A., and Stossel, T. P. (1987) *Nature* **325**, 362-364
92. Lassing, I., and Lindberg, U. (1985) *Nature* **314**, 472-474
93. Gorbatyuk, V. Y., Nosworthy, N. J., Robson, S. A., Bains, N. P. S., Maciejewski, M. W., dos Remedios, C. G., and King, G. F. (2006) *Molecular Cell* **24**, 511-522
94. Ishihara, H., Shibasaki, Y., Kizuki, N., Katagiri, H., Yazaki, Y., Asano, T., and Oka, Y. (1996) *J. Biol. Chem.* **271**, 23611-23614
95. Loijens, J. C., and Anderson, R. A. (1996) *J. Biol. Chem.* **271**, 32937-32943
96. Giudici, M.-L., Emson, P. C., and Irvine, R. F. (2004) *Biochem. J.* **379**, 489-496

97. Wang, L., Li, G., and Sugita, S. (2005) *J. Biol. Chem.* **280**, 16522-16527
98. Stace, C., Manifava, M., Delon, C., Coadwell, J., Cockcroft, S., and Ktistakis, N. T. (2008) *Adv Enzyme Regul* **48**, 55-72
99. Skippen, A., Jones, D. H., Morgan, C. P., Li, M., and Cockcroft, S. (2002) *J. Biol. Chem.* **277**, 5823-5831
100. Luo, B., Prescott, S. M., and Topham, M. K. (2004) *Cellular Signalling* **16**, 891-897
101. Yamamoto, M., Chen, M. Z., Wang, Y. J., Sun, H. Q., Wei, Y., Martinez, M., and Yin, H. L. (2006) *J Biol Chem* **281**, 32630-32638
102. Chong, L. D., Traynor-Kaplan, A., Bokoch, G. M., and Schwartz, M. A. (1994) *Cell* **79**, 507-513
103. Weernink, P. A. O., Meletiadis, K., Hommeltenberg, S., Hinz, M., Ishihara, H., Schmidt, M., and Jakobs, K. H. (2004) *J. Biol. Chem.* **279**, 7840-7849
104. Honda, A., Nogami, M., Yokozeki, T., Yamazaki, M., Nakamura, H., Watanabe, H., Kawamoto, K., Nakayama, K., Morris, A. J., Frohman, M. A., and Kanaho, Y. (1999) *Cell* **99**, 521-532
105. Shin, N., Ahn, N., Chang-Ileto, B., Park, J., Takei, K., Ahn, S. G., Kim, S. A., Di Paolo, G., and Chang, S. (2008) *J Cell Sci* **121**, 1252-1263
106. Shinozaki-Narikawa, N., Kodama, T., and Shibasaki, Y. (2006) *Traffic* **7**, 1539-1550
107. Rozelle, A. L., Machesky, L. M., Yamamoto, M., Driessens, M. H. E., Insall, R. H., Roth, M. G., Luby-Phelps, K., Marriott, G., Hall, A., and Yin, H. L. (2000) *Current Biology* **10**, 311-320
108. Boronenkov, I. V., Loijens, J. C., Umeda, M., and Anderson, R. A. (1998) *Mol. Biol. Cell* **9**, 3547-3560
109. Chatah, N. E., and Abrams, C. S. (2001) *J Biol Chem* **276**, 34059-34065
110. Doughman, R. L., Firestone, A. J., and Anderson, R. A. (2003) *Journal of Membrane Biology* **194**, 77-89
111. Santarius, M., Lee, C. H., and Anderson, R. A. (2006) *Biochem J* **398**, 1-13
112. Kisseleva, M., Feng, Y., Ward, M., Song, C., Anderson, R. A., and Longmore, G. D. (2005) *Mol. Cell. Biol.* **25**, 3956-3966
113. Arioka, M., Nakashima, S., Shibasaki, Y., and Kitamoto, K. (2004) *Biochemical and Biophysical Research Communications* **319**, 456-463
114. Kunz, J., Wilson, M. P., Kisseleva, M., Hurley, J. H., Majerus, P. W., and Anderson, R. A. (2000) *Molecular Cell* **5**, 1-11
115. Audhya, A., Loewith, R., Parsons, A. B., Gao, L., Tabuchi, M., Zhou, H., Boone, C., Hall, M. N., and Emr, S. D. (2004) *Embo J* **23**, 3747-3757
116. Stefan, D., Baird, D., Ling, Y., Audhya, A., and Emr, S. (2006) *Mol Cell Biol* **17 (suppl)**, 2493. (CD-ROM)
117. Desrivieres, S., Cooke, F. T., Parker, P. J., and Hall, M. N. (1998) *J. Biol. Chem.* **273**, 15787-15793
118. Deng, L., Sugiura, R., Ohta, K., Tada, K., Suzuki, M., Hirata, M., Nakamura, S.-i., Shuntoh, H., and Kuno, T. (2005) *J. Biol. Chem.* **280**, 27561-27568
119. Zhang, Y., Sugiura, R., Lu, Y., Asami, M., Maeda, T., Itoh, T., Takenawa, T., Shuntoh, H., and Kuno, T. (2000) *J. Biol. Chem.* **275**, 35600-35606

120. Hassan, B. A., Prokopenko, S. N., Breuer, S., Zhang, B., Paululat, A., and Bellen, H. J. (1998) *Genetics* **150**, 1527-1537
121. Cheng, M. K., and Shearn, A. (2004) *Genetics* **167**, 1213-1223
122. Perdigoto, C. N., Gervais, L., Overstreet, E., Fischer, J., Guichet, A., and Schweisguth, F. (2008) *PLoS ONE* **3**, e3072
123. Gervais, L., Claret, S., Januschke, J., Roth, S., and Guichet, A. (2008) *Development* **135**, 3829-3838
124. Compagnon, J., Gervais, L., Roman, M. S., Chamot-Boeuf, S., and Guichet, A. (2009) *J Cell Sci* **122**, 25-35
125. Wei, H. C., Rollins, J., Fabian, L., Hayes, M., Polevoy, G., Bazinet, C., and Brill, J. A. (2008) *J Cell Sci* **121**, 1076-1084
126. Shibasaki, Y., Ishihara, H., Kizuki, N., Asano, T., Oka, Y., and Yazaki, Y. (1997) *J. Biol. Chem.* **272**, 7578-7581
127. Matsui, T., Yonemura, S., Tsukita, S., and Tsukita, S. (1999) *Current Biology* **9**, 1259-1265
128. Powner, D. J., Payne, R. M., Pettitt, T. R., Giudici, M. L., Irvine, R. F., and Wakelam, M. J. O. (2005) *J Cell Sci* **118**, 2975-2986
129. Galiano, F. J., Ulug, E. T., and Davis, J. N. (2002) *J Cell Biochem* **85**, 131-145
130. Barbieri, M. A., Heath, C. M., Peters, E. M., Wells, A., Davis, J. N., and Stahl, P. D. (2001) *J. Biol. Chem.* **276**, 47212-47216
131. Ling, K., Bairstow, S. F., Carbonara, C., Turbin, D. A., Huntsman, D. G., and Anderson, R. A. (2007) *J Cell Biol* **176**, 343-353
132. Yamamoto, M., Hilgemann, D. H., Feng, S., Bito, H., Ishihara, H., Shibasaki, Y., and Yin, H. L. (2001) *J. Cell Biol.* **152**, 867-876
133. Tolias, K., and Carpenter, C. L. (2000) *Methods Enzymol* **325**, 190-200
134. Wong, K.-W., and Isberg, R. R. (2003) *J. Exp. Med.* **198**, 603-614
135. Auvinen, E., Kivi, N., and Vaheri, A. (2007) *Exp Cell Res* **313**, 824-833
136. Yamazaki, M., Miyazaki, H., Watanabe, H., Sasaki, T., Maehama, T., Frohman, M. A., and Kanaho, Y. (2002) *J. Biol. Chem.* **277**, 17226-17230
137. Aikawa, Y., and Martin, T. F. J. (2003) *J. Cell Biol.* **162**, 647-659
138. Doughman, R. L., Firestone, A. J., Wojtasiak, M. L., Bunce, M. W., and Anderson, R. A. (2003) *J Biol Chem* **278**, 23036-23045
139. Davis, J. N., Rock, C. O., Cheng, M., Watson, J. B., Ashmun, R. A., Kirk, H., Kay, R. J., and Roussel, M. F. (1997) *Mol. Cell. Biol.* **17**, 7398-7406
140. Shyng, S. L., Barbieri, A., Gumusboga, A., Cukras, C., Pike, L., Davis, J. N., Stahl, P. D., and Nichols, C. G. (2000) *PNAS* **97**, 937-941
141. Tolias, K. F., Hartwig, J. H., Ishihara, H., Shibasaki, Y., Cantley, L. C., and Carpenter, C. L. C. L. (2000) *Current Biology* **10**, 153-156
142. Guerriero, C. J., Weixel, K. M., Bruns, J. R., and Weisz, O. A. (2006) *J. Biol. Chem.* **281**, 15376-15384
143. van Horck, F. P. G., Lavazais, E., Eickholt, B. J., Moolenaar, W. H., and Divecha, N. (2002) *Current Biology* **12**, 241-245
144. Greenberg, S. (1999) *J Leukoc Biol* **66**, 712-717
145. Bairstow, S. F., Ling, K., Su, X., Firestone, A. J., Carbonara, C., and Anderson, R. A. (2006) *J. Biol. Chem.* **281**, 20632-20642

146. Lacalle, R. A., Peregil, R. M., Albar, J. P., Merino, E., Martinez, A. C., Merida, I., and Manes, S. (2007) *J Cell Biol* **179**, 1539-1553
147. Lokuta, M. A., Senetar, M. A., Bennin, D. A., Nuzzi, P. A., Chan, K. T., Ott, V. L., and Huttenlocher, A. (2007) *Mol Biol Cell* **18**, 5069-5080
148. Oude Weernink, P. A., Schmidt, M., and Jakobs, K. H. (2004) *European Journal of Pharmacology* **500**, 87-99
149. Tolias, K. F., Cantley, L. C., and Carpenter, C. L. (1995) *J. Biol. Chem.* **270**, 17656-17659
150. Tolias, K. F., Couvillon, A. D., Cantley, L. C., and Carpenter, C. L. (1998) *Mol. Cell. Biol.* **18**, 762-770
151. Oude Weernink, P. A., Meletiadis, K., Hommeltenberg, S., Hinz, M., Ishihara, H., Schmidt, M., and Jakobs, K. H. (2004) *J Biol Chem* **279**, 7840-7849
152. Divecha, N., Roefs, M., Halstead, J. R., D'Andrea, S., Fernandez-Borga, M., Wakelam, M. J. O., and D'Santos, C. (2000) *EMBO J.* **19**, 5440-5449
153. Schmidt, M., RÃ¼menapp, U., Nehls, C., Ott, S., Keller, J., von Eichel-Streiber, C., and Jakobs, K. H. (1996) *European Journal of Biochemistry* **240**, 707-712
154. Krauss, M., Kinuta, M., Wenk, M. R., De Camilli, P., Takei, K., and Haucke, V. (2003) *J. Cell Biol.* **162**, 113-124
155. Boronenkov, I. V., and Anderson, R. A. (1995) *J. Biol. Chem.* **270**, 2881-2884
156. Rumenapp, U., Schmidt, M., Olesch, S., Ott, S., Eichel-Streiber, C. V., and Jakobs, K. H. (1998) *Biochem J* **334 (Pt 3)**, 625-631
157. Mesaeli, N., Tappia, P. S., Suzuki, S., Dhalla, N. S., and Panagia, V. (2000) *Archives of Biochemistry and Biophysics* **382**, 48-56
158. Gong, L.-W., Di Paolo, G., Diaz, E., Cestra, G., Diaz, M.-E., Lindau, M., De Camilli, P., and Toomre, D. (2005) *PNAS* **102**, 5204-5209
159. Mao, Y. S., Yamaga, M., Zhu, X., Wei, Y., Sun, H. Q., Wang, J., Yun, M., Wang, Y., Di Paolo, G., Bennett, M., Mellman, I., Abrams, C. S., De Camilli, P., Lu, C. Y., and Yin, H. L. (2009) *J Cell Biol* **184**, 281-296
160. Wenk, M. R., Pellegrini, L., Klenchin, V. A., Di Paolo, G., Chang, S., Daniell, L., Arioka, M., Martin, T. F., and De Camilli, P. (2001) *Neuron* **32**, 79-88
161. Hynes, R. O. (2002) *Cell* **110**, 673-687
162. Chandrasekar, I., Stradal, T. E. B., Holt, M. R., Entschladen, F., Jockusch, B. M., and Ziegler, W. H. (2005) *J Cell Sci* **118**, 1461-1472
163. Saunders, R. M., Holt, M. R., Jennings, L., Sutton, D. H., Barsukov, I. L., Bobkov, A., Liddington, R. C., Adamson, E. A., Dunn, G. A., and Critchley, D. R. (2006) *European Journal of Cell Biology* **85**, 487-500
164. Critchley, D. R. (2005) *Biochem. Soc. Trans.* **33**, 1308-1312
165. Martel, V., Racaud-Sultan, C., Dupe, S., Marie, C., Paulhe, F., Galmiche, A., Block, M. R., and Albiges-Rizo, C. (2001) *J. Biol. Chem.* **276**, 21217-21227
166. Cremona, O., Di Paolo, G., Wenk, M. R., Luthi, A., Kim, W. T., Takei, K., Daniell, L., Nemoto, Y., Shears, S. B., Flavell, R. A., McCormick, D. A., and De Camilli, P. (1999) *Cell* **99**, 179-188
167. Narkis, G., Ofir, R., Landau, D., Manor, E., Volokita, M., Hershkowitz, R., Elbedour, K., and Birk, O. S. (2007) *Am J Hum Genet* **81**, 530-539

168. Morgan, J. R., Di Paolo, G., Werner, H., Shchedrina, V. A., Pypaert, M., Pieribone, V. A., and De Camilli, P. (2004) *J. Cell Biol.* **167**, 43-50
169. Honing, S., Ricotta, D., Krauss, M., Spate, K., Spolaore, B., Motley, A., Robinson, M., Robinson, C., Haucke, V., and Owen, D. J. (2005) *Molecular Cell* **18**, 519-531
170. Krauss, M., Kukhtina, V., Pechstein, A., and Haucke, V. (2006) *PNAS* **103**, 11934-11939
171. Heldwein, E. E., Macia, E., Wang, J., Yin, H. L., Kirchhausen, T., and Harrison, S. C. (2004) *PNAS* **101**, 14108-14113
172. Akiyama, C., Shinozaki-Narikawa, N., Kitazawa, T., Hamakubo, T., Kodama, T., and Shibasaki, Y. (2005) *Cell Biol Int* **29**, 514-520
173. El Sayegh, T. Y., Arora, P. D., Ling, K., Laschinger, C., Janmey, P. A., Anderson, R. A., and McCulloch, C. A. (2007) *Mol Biol Cell* **18**, 3026-3038
174. Delmas, P., Crest, M., and Brown, D. A. (2004) *Trends in Neurosciences* **27**, 41-47
175. Koreh, K., and Monaco, M. E. (1986) *J. Biol. Chem.* **261**, 88-91
176. Nakanishi, S., Catt, K. J., and Balla, T. (1995) *PNAS* **92**, 5317-5321
177. Ridley, A. J. (2001) *Trends in Cell Biology* **11**, 471-477
178. Arora, P. D., Chan, M. W. C., Anderson, R. A., Janmey, P. A., and McCulloch, C. A. (2005) *Mol. Biol. Cell* **16**, 5175-5190
179. Nelson, C. D., Kovacs, J. J., Nobles, K. N., Whalen, E. J., and Lefkowitz, R. J. (2008) *J Biol Chem* **283**, 21093-21101
180. Xie, Z., Chang, S. M., Pennypacker, S. D., Liao, E. Y., and Bikle, D. D. (2009) *Mol Biol Cell*
181. Emoto, K., Inadome, H., Kanaho, Y., Narumiya, S., and Umeda, M. (2005) *J. Biol. Chem.* **280**, 37901-37907
182. Field, S. J., Madson, N., Kerr, M. L., Galbraith, K. A., Kennedy, C. E., Tahiliani, M., Wilkins, A., and Cantley, L. C. (2005) *Curr Biol* **15**, 1407-1412
183. Bunce, M. W., Bergendahl, K., and Anderson, R. A. (2006) *Biochimica et Biophysica Acta (BBA) - Molecular and Cell Biology of Lipids* **1761**, 560-569
184. Mortier, E., Wuytens, G., Leenaerts, I., Hannes, F., Heung, M. Y., Degeest, G., David, G., and Zimmermann, P. (2005) *Embo J* **24**, 2556-2565
185. Yu, H., Fukami, K., Watanabe, Y., Ozaki, C., and Takenawa, T. (1998) *Eur J Biochem* **251**, 281-287
186. Ho, K. K., Anderson, A. A., Rosivatz, E., Lam, E. W., Woscholski, R., and Mann, D. J. (2008) *J Biol Chem* **283**, 5477-5485
187. Kakuk, A., Friedlander, E., Vereb, G., Jr., Kasa, A., Balla, A., Balla, T., Heilmeyer, L. M., Jr., Gergely, P., and Vereb, G. (2006) *Cytometry A* **69**, 1174-1183
188. Mellman, D. L., Gonzales, M. L., Song, C., Barlow, C. A., Wang, P., Kendziorski, C., and Anderson, R. A. (2008) *Nature* **451**, 1013-1017
189. Audhya, A., and Emr, S. D. (2003) *Embo J* **22**, 4223-4236
190. Garcia-Garcia, E., and Rosales, C. (2002) *J. Leukoc. Biol.* **72**, 1092-1108
191. Sobota, A., Strzelecka-Kiliszek, A., Gladkowska, E., Yoshida, K., Mrozinska, K., and Kwiatkowska, K. (2005) *J. Immunol.* **175**, 4450-4457

192. Cox, D., and Greenberg, S. (2001) *Semin Immunol* **13**, 339-345
193. Gupta, N., Wollscheid, B., Watts, J. D., Scheer, B., Aebersold, R., and DeFranco, A. L. (2006) *Nat Immunol* **7**, 625-633
194. Hao, S., and August, A. (2005) *Mol Biol Cell* **16**, 2275-2284
195. Andrews, N. L., Lidke, K. A., Pfeiffer, J. R., Burns, A. R., Wilson, B. S., Oliver, J. M., and Lidke, D. S. (2008) *Nature cell biology* **10**, 955-963
196. Kaizuka, Y., Douglass, A. D., Varma, R., Dustin, M. L., and Vale, R. D. (2007) *Proceedings of the National Academy of Sciences of the United States of America* **104**, 20296-20301
197. May, R. C., Caron, E., Hall, A., and Machesky, L. M. (2000) *Nature Cell. Biol.* **2**, 246-248
198. Labno, C. M., Lewis, C. M., You, D., Leung, D. W., Takesono, A., Kamberos, N., Seth, A., Finkelstein, L. D., Rosen, M. K., Schwartzberg, P. L., and Burkhardt, J. K. (2003) *Current biology* **13**, 1619-1624
199. Bonnerot, C., Briken, V., Brachet, V., Lankar, D., Cassard, S., Jabri, B., and Amigorena, S. (1998) *The EMBO journal* **17**, 4606-4616
200. Hall, A. B., Gakidis, M. A., Glogauer, M., Wilsbacher, J. L., Gao, S., Swat, W., and Brugge, J. S. (2006) *Immunity* **24**, 305-316
201. Cox, D., Chang, P., Kurosaki, T., and Greenberg, S. (1996) *J. Biol. Chem.* **271**, 16597-16602
202. Tskvitaria-Fuller, I., Mistry, N., Sun, S., and Wulfing, C. (2007) *J Immunol Methods* **319**, 64-78
203. Wells, C. M., Walmsley, M., Ooi, S., Tybulewicz, V., and Ridley, A. J. (2004) *J. Cell. Sci.* **117**, 1259-1268
204. Caron, E., and Hall, A. (1998) *Science (New York, N.Y* **282**, 1717-1721
205. Kaplan, G. (1977) *Scand J Immunol* **6**, 797-807
206. Olazabal, I. M., Caron, E., May, R. C., Schilling, K., Knecht, D. A., and Machesky, L. M. (2002) *Curr Biol* **12**, 1413-1418
207. Griffin, F. M., Jr., and Silverstein, S. C. (1974) *J Exp Med* **139**, 323-336
208. Ozaki, S., DeWald, D. B., Shope, J. C., Chen, J., and Prestwich, G. D. (2000) *PNAS* **97**, 11286-11291
209. Muallem, S., Kwiatkowska, K., Xu, X., and Yin, H. L. (1995) *J Cell Biol* **128**, 589-598
210. Burridge, K., and Wennerberg, K. (2004) *Cell* **116**, 167-179
211. Wheeler, A. P., Wells, C. M., Smith, S. D., Vega, F. M., Henderson, R. B., Tybulewicz, V. L., and Ridley, A. J. (2006) *J. Cell. Sci.* **119**, 2749-2757
212. Yeung, T., Ozdamar, B., Paroutis, P., and Grinstein, S. (2006) *Current Opinion in Cell Biology* **18**, 429-437
213. Lorenzi, R., Brickell, P. M., Katz, D. R., Kinnon, C., and Thrasher, A. J. (2000) *Blood* **95**, 2943-2946
214. Rohatgi, R., Ma, L., Miki, H., Lopez, M., Kirchhausen, T., Takenawa, T., and Kirschner, M. W. (1999) *Cell* **97**, 221-231
215. Takenawa, T., and Suetsugu, S. (2007) *Nat Rev Mol Cell Biol* **8**, 37-48
216. Pixley, F. J., and Stanley, E. R. (2004) *Trends Cell Biol* **14**, 628-638

217. Downey, G. P., Botelho, R. J., Butler, J. R., Moltyaner, Y., Chien, P., Schreiber, A. D., and Grinstein, S. (1999) *J. Biol. Chem.* **274**, 28436-28444
218. Miah, S. M., Sada, K., Tuazon, P. T., Ling, J., Maeno, K., Kyo, S., Qu, X., Tohyama, Y., Traugh, J. A., and Yamamura, H. (2004) *Molecular and cellular biology* **24**, 71-83
219. Kusumi, A., Nakada, C., Ritchie, K., Murase, K., Suzuki, K., Murakoshi, H., Kasai, R. S., Kondo, J., and Fujiwara, T. (2005) *Annu Rev Biophys Biomol Struct* **34**, 351-378
220. Villalba, M., Bi, K., Rodriguez, F., Tanaka, Y., Schoenberger, S., and Altman, A. (2001) *J Cell Biol* **155**, 331-338
221. Garcia-Garcia, E., Brown, E. J., and Rosales, C. (2007) *J Immunol* **178**, 3048-3058
222. Kawasaki, M., Shiba, T., Shiba, Y., Yamaguchi, Y., Matsugaki, N., Igarashi, N., Suzuki, M., Kato, R., Kato, K., Nakayama, K., and Wakatsuki, S. (2005) *Genes to Cells* **10**, 639-654
223. Hackam, D. J., Rotstein, O. D., Schreiber, A., Zhang, W., and Grinstein, S. (1997) *J. Exp. Med.* **186**, 955-966
224. Ren, X. D., Bokoch, G. M., Traynor-Kaplan, A., Jenkins, G. H., Anderson, R. A., and Schwartz, M. A. (1996) *Molecular biology of the cell* **7**, 435-442
225. Continolo, S., Baruzzi, A., Majeed, M., Caveggion, E., Fumagalli, L., Lowell, C. A., and Berton, G. (2005) *Exp Cell Res* **302**, 253-269
226. Lee, W. L., Cosio, G., Ireton, K., and Grinstein, S. (2007) *J. Biol. Chem.* **282**, 11135-11143